

**INVESTIGATING NOVEL MACROMOLECULAR GEOMETRIES  
UTILIZING THE COILED-COIL PEPTIDE MOTIF**

by

Grant Alexander Knappe

A thesis submitted to the Faculty of the University of Delaware in partial fulfillment of the requirements for the degree of Honors Bachelor of Chemical Engineering with Distinction

Spring 2019

© 2019 Grant Alexander Knappe  
All Rights Reserved

**INVESTIGATING NOVEL MACROMOLECULAR GEOMETRIES  
UTILIZING THE COILED-COIL PEPTIDE MOTIF**

by

Grant Alexander Knappe

Approved: \_\_\_\_\_  
Christopher J. Kloxin, Ph.D.  
Professor in charge of thesis on behalf of the Advisory Committee

Approved: \_\_\_\_\_  
Thomas H. Epps III, Ph.D.  
Committee member from the Department of Chemical & Biomolecular  
Engineering

Approved: \_\_\_\_\_  
Susan E. Groh, Ph. D.  
Committee member from the Board of Senior Thesis Readers

Approved: \_\_\_\_\_  
Earl Lee II, Ph.D  
Deputy Faculty Director, University Honors Program

## ACKNOWLEDGMENTS

The University of Delaware has provided an enriching and challenging environment to forge me into the scientist, scholar, and person that I am today. It has also instilled values that will allow for my continued growth in those. Perhaps the most important factor that the University of Delaware has provided me is the collection of amazing people I have shared my life with.

First, I need to acknowledge Dr. Christopher Kloxin. After emailing ten professors in the fall of my freshman year, he was the only professor that emailed me back to set up a meeting but also took a chance on me joining his laboratory. Since then, he has been immensely supportive in my pursuits in research and school, and he continues to teach me lessons as a scientist and as a person. The conversations we have shared have challenged and enriched my understanding of science, and his continual support has afforded me many opportunities to advance my career. I wish I was an English major in order to fully describe the impact he has had on me, but if that were the case, we probably would not have met. Thank you for all your insight and advice over the past four years. I also want to acknowledge Dr. Thomas Epps III and Dr. Susan Groh. Both have been great committee members, have taught me core courses in my education, and have generously supported me in opportunities that I pursued.

None of the work presented in this thesis would be possible without the group of great people in the Kloxin group. First, I want to thank Dr. Melissa Gordon and Dr. Abhishek Shete, who trained me into the scientist and researcher I am today. Always

encouraging and supportive, both were fantastic mentors and were instrumental in my development. I also want to thank Nicole Halaszynski and Bryan Sutherland, for training on various techniques used in this thesis as well as preparing many of the samples mentioned in this work. Specifically, Bryan Sutherland synthesized the small molecule ATRP initiator used in chapter 3, and helped obtain all of the MALDI data. In addition, Nicole Halaszynski synthesized and purified many of the peptides used in both chapters 2 and 3, and conducted the stabilization studies in chapter 2. Again, the training and coloration were much appreciated during this busy final year in university. I also want to thank all of the Kloxin group members that have passed through the lab over the years I was there, especially Dr. Bassil El-Zaatari, and Mukund Kabra, who have been best of friends and made coming to lab a little more exciting (or less discouraging).

I want to thank the faculty and the support staff in the Chemical & Bimolecular Engineering department for creating an incredible environment for undergraduates to learn and to research. The collective effort to pursue the best pedagogy positively affected my life and many others around me.

I want to thank those around me that push me to do the work I do every day. To Steve, Justin, Fernando, Ben, Trent, and Allan: it has been a meaningful experience working, living, or relaxing with you. The memories of the hard work and long nights will fade slowly, and it was my pleasure to obtain this degree with you. To Alex, Brendan, Kondwani, and others: your friendship and time during the weekdays and weekends were necessary and appreciated for me to stay calm and relaxed during my time at UD. To my friends from before UD, especially Jake, Evan, Kevin, Nick, and Ann: thank you for visiting me here at UD and for inviting me to your colleges. Those

weekends are some of my best memories during my time, and I always appreciated being able to talk to you about what I was going through at UD. All of the people I mentioned helped me appreciate the good times, and helped me get through the bad times.

Finally, I want to acknowledge my family. To my brother, I hope that I have set a great example to follow, and that you accomplish whatever you want to accomplish during your time in college, while still having some fun. To my parents: you have both been incredibly supportive when I am down, and the best fans when I succeed. Only through your support and sacrifices have I been able to reach where I am today, and my words do not adequately show my appreciation. Thank you for everything.

## TABLE OF CONTENTS

LIST OF TABLES .....	viii
LIST OF FIGURES .....	ix
ABSTRACT .....	xiii

### Chapter

1	INTRODUCTION .....	1
1.1	Biomimicry for Material Design.....	1
1.2	The Coiled-Coil Peptide Motif .....	3
1.3	Solid-State Peptide Synthesis .....	5
1.4	Macromolecular Design Chemistries.....	7
1.5	Dynamic Hydrogels .....	10
1.6	Thesis Overview .....	10
2	COVALENT STABILIZATION OF THE COILED-COIL MOTIF.....	12
2.1	Introduction.....	12
2.2	Materials and Experimental Methods .....	14
2.2.1	Monomer Synthesis .....	14
2.2.2	Peptide Synthesis .....	14
2.2.3	Peptide Purification .....	15
2.2.4	Conjugation Conditions.....	16
2.2.5	Characterization.....	16
2.3	Results and Discussion .....	17
2.4	Summary and Conclusions .....	19
3	SYNTHESIS OF POLYMER-PEPTIDE CONJUGATES WITH STAR GEOMETRIES.....	20
3.1	Introduction.....	20
3.2	Materials and Experimental Methods .....	22
3.2.1	Peptide Synthesis .....	22
3.2.2	Monomer Synthesis .....	23
3.2.3	Peptide Purification .....	23
3.2.4	Grafting-from Polymerization Conditions .....	24
3.2.5	Characterization.....	24
3.3	Results and Discussion .....	25

3.4	Summary and Conclusions .....	38
4	CONCLUSIONS AND FUTURE DIRECTIONS.....	39
4.1	Conclusions.....	39
4.2	Future Directions – Physical Behavior of Novel Macromolecular Geometries .....	40
4.3	Future Directions - Multi-Stimuli Responsive Hydrogels .....	42
	REFERENCES .....	44
Appendix		
A	PEPETIDE SEQUENCES.....	47
B	SUPPORTING INFORMATION: COVALENT STABILIZATION OF THE COILED-COIL MOTIF.....	48
C	SUPPORTING INFORMATION: SYNTHESIS OF POLYMER-PEPTIDE CONJUGATES WITH STAR GEOMETRIES .....	51

## LIST OF TABLES

Table 1	Reaction tables detailing ATRP conditions for synthesis of star polymer-peptide conjugates. Typical procedure details are described in chapter 3.2.4. Unless otherwise specified, the initiator is the small molecule ATRP initiator, and the solvent is D <sub>2</sub> O.....	28
Table 2	Peptide sequences used with corresponding experimental relevance .....	47
Table 3	CuAAC reaction conditions for covalent stabilization of coiled-coil assembly .....	48

## LIST OF FIGURES

- Figure 1 A version of the coiled-coil peptide motif showing an anti-parallel homotetrameric collection of  $\alpha$ -helices. The peptide sequence is characterized by the heptadic repeat unit *abcdefg*. The amino acids *a* and *d* are hydrophobic and are hidden towards the inner core of the assembly. Amino acids *e* and *g* are hydrophilic in nature and provide complimentary interactions that stabilize the assembly. The amino acids *b*, *c*, and *f* are often exchangeable and are not important in the assembly of this peptide motif. C and N denote the carbon and nitrogen termini of the peptides..... 4
- Figure 2 The iterative approach to generating polypeptides on a solid-state support. An amine functionalized resin reacts with a amine-protected amino acid, generating the first residue in the sequence. Then, piperidine removes the Fmoc group to reveal an amine that can react to the next protected amino acid. The final polypeptide design is then cleaved from the solid support using trifluoroacetic acid. .... 6
- Figure 3 The mechanism for polymer synthesis via atom transfer radical polymerization. When an initiator is initiated, a primary vinyl monomer is added via normal radical polymerization. The growing radical can either add another monomer, or deactivate via the addition of a halogen adduct. Once deactivated, the growing chain will not add another monomer until it is activated, in which case it can proceed to add another monomer via a radical addition. The equilibrium defined by the activation and deactivation controls the kinetics of the polymerization. .... 8
- Figure 4 Schematic showing the covalent stabilization hypothesized. A peptide functionalized on both termini with a special chemical moiety self assembles to form a coiled-coil bundle with four reactive handles on the top and bottom of the assembly. A tetra-functionalized small molecule can react to the peptide to covalently lock the assembly architecture. .... 13
- Figure 5 CD spectrum of the diazide peptide. The typical minima at 208 nm and 222 nm are indicative of the assembly of the diazide peptides into coiled-coil bundles..... 18
- Figure 6 The proposed star geometry polymer-peptide conjugate using aqueous ATRP to control the polymerization of the growing chains off of the peptide. Once generated, this star polymer-peptide conjugate will have a dynamic central linkage that will respond to thermal stimulus. .... 21

Figure 7	The synthetic route to obtain an ATRP-macrinitiator. Alloc-group deprotection of a centrally located lysine is performed, generating a free lysine that is able to subsequently react. The amide bond formed generates an ATRP-macroinitiator. When self-assembled, each bundle should have four initiating units, all on the outside of the assembly. ....	26
Figure 8	Circular Dichroic spectra of A) 4459-a-Br and B) p622-Br. P622-Br does not assembly into coiled-coil bundles. The 4459-a-Br assembles like its parent peptide, but its melting behavior shows that it is less thermodynamically stable.....	27
Figure 9	The NMR spectrum of R <sub>95</sub> -2. Peaks at 5.67 and 6.10 ppm are protons of the double bond of the monomer. Peaks at 1.07 and 0.87 ppm are methyl protons generated during the polymerization. ....	30
Figure 10	The MALDI spectrum for R <sub>98</sub> -3.....	31
Figure 11	The MALDI spectrum for R <sub>100</sub> -4. Molecular weight of the base macroinitiator is 3753 Da. The peak around 7500 Da is hypothesized to be the +2 charged species of the macroinitiator. ....	32
Figure 12	MALDI spectra of A) R <sub>102</sub> -1 and B) R <sub>102</sub> -2, along with the reference peaks of the base peptide. The spectra do not show the formation of a new population centered at the target molecular weight. ....	34
Figure 13	CD spectra showing the effects of initiator chain extension of the assembly behavior of the coiled-coil peptides. A) base peptide 4459-a-Br. B) 4459-a-E-Br. C) 4459-a-EG-Br. D) 4459-a-EGE-Br. Moving the bromide initiator group just one amino acid away from the base peptide sequence significantly increases the thermodynamic stability of the coiled-coil bundle. Additional amino acid additions show slight improvements. The increase in thermodynamic stability is hypothesized as resulting from the decrease in side chain interference with the inside assembly environment. ....	35
Figure 14	MALDI spectra of A) R <sub>104</sub> -1 B) R <sub>104</sub> -2 C)R <sub>104</sub> -3. While the chain extensions of the initiator proved to increase coiled-coil stability, there are no improvements in the polymerization conditions. For each of these reactions, the desired molecular weight was 18000 Da. This new population does not appear in the MALDI spectra. ....	36
Figure 15	MALDI spectra of R <sub>106</sub> . All reactions targeted a molecular weight of 15 kDa. A) Typical reaction conditions B) PMDETA as the copper ligand C) BiPy as the copper ligand D) 50 mM sodium bromide .....	37

Figure 16	Reaction schematic detailing the synthesis of a cross-linked hydrogel incorporating the polymer-peptide conjugates. A flexible and hydrophilic tetrathiol could react with the prepared start conjugates to generate a crosslinked hydrogel, where the chemical crosslinks are generated by a thiol-X nucleophilic attack reaction. The physical crosslinks are the coiled-coil peptide assembly, which have temperature dependent behavior.....	42
Figure 17	NMR spectrum of the tetraalkyne small molecule used for covalent stabilization.....	49
Figure 18	Chromatograph and corresponding mass spectra for the first covalent stabilization reaction attempt.....	50
Figure 19	Chromatograph and corresponding mass spectra for the second covalent stabilization reaction attempt. ....	50
Figure 20	NMR spectrum of the small molecule initiator used in the model polymerizations (sample prepared in deuterated DMSO). ....	51
Figure 21	NMR spectrum of R <sub>95-1</sub> . ....	52
Figure 22	NMR spectrum of R <sub>95-3</sub> .....	52
Figure 23	NMR spectrum of R <sub>95-4</sub> .....	53
Figure 24	NMR spectrum of R <sub>98-1</sub> .....	53
Figure 25	NMR spectrum of R <sub>98-2</sub> .....	54
Figure 26	NMR spectrum of R <sub>98-3</sub> .....	54
Figure 27	NMR spectrum of R <sub>100-1</sub> .....	55
Figure 28	NMR spectrum of R <sub>100-2</sub> .....	55
Figure 29	NMR spectrum of R <sub>100-4</sub> .....	56
Figure 30	NMR spectrum of R <sub>102-1</sub> .....	56
Figure 31	NMR spectrum of R <sub>102-2</sub> .....	57
Figure 32	NMR spectrum of R <sub>102-3</sub> .....	57
Figure 33	NMR spectrum of R <sub>104-1</sub> .....	58

Figure 34	NMR spectrum of R <sub>104</sub> -2 .....	58
Figure 35	NMR spectrum of R <sub>104</sub> -3 .....	59

## ABSTRACT

The synthesis of novel macromolecular geometries enables an expanded understanding of the synthesis, physics, and applications of these materials. This work explores the design and synthesis of novel geometries using the coiled-coil peptide motif as a building block. Covalent stabilization of the coiled-coil peptide motif at the top and the bottom of the assembly was pursued to generate a spherical macromolecule. The required peptides and small molecule capping molecule were prepared; however, the precise conjugation necessary to develop this geometry was not successful. Instead, it appears that the small molecule crosslinks peptides from different assemblies together. Some secondary forces to pattern/anchor the molecules during the conjugation may be necessary to synthesize the desired geometry.

A novel star geometry polymer-peptide conjugate was synthesized using a grafting-from approach, again utilizing a coiled-coil peptide assembly as the base of the macromolecule. A library of ATRP-functionalized peptides was synthesized that assemble into the coiled-coil motif with ATRP initiators decorating the outside of the assembly. Extending the ATRP initiator away from the peptide, and therefore the assembly, proves to increase the stability of the assembly. Model ATRP polymerization studies were conducted on a small molecule to determine the best polymerization procedures for our target monomer. Many attempts at synthesizing the target polymer-peptide conjugate proceeded in an uncontrollable manner that was characterized unsuccessfully. Improvements to the polymerizations were made, but the synthesis of well-defined star shaped polymer-peptide conjugates was unsuccessful.

## Chapter 1

### INTRODUCTION

#### 1.1 Biomimicry for Material Design

The natural world around us has developed complex materials to solve the fundamental engineering problems that we face today. One example that highlights nature's ingenuity are butterfly wings. Saturated, rich colors are desired in nature for many reasons, and the solution to creating these colors is completely different to how we create colors. Instead of environmentally harmful dyes, nature uses nanostructured materials to generate iridescence of sunlight, resulting in beautiful colors. In various butterfly wings, cryptic coloration and intraspecies communication are accomplished through nanostructured and nano-oriented multilayered materials that generate robust iridescent coloring.<sup>1</sup> Another example of nature utilizing microstructure for improved material performance is found in the alien world of the deep ocean, where ancient predators called sharks live. Their skin is patterned with dermal denticles that reduces the drag fast-swimming sharks experience when traveling, saving energy and improving performance.<sup>2</sup> In both cases, various engineering efforts have been made towards developing synthetic versions of the natural structure and function.<sup>3-6</sup>

In addition to nanostructured materials that impart functionality, nature has also mastered multi-length scale patterns to generate functionality. Perhaps the most famous example is of the gecko's foot. Many scientists pondered the forces and mechanism behind the incredible adhesive performance observed by a gecko's foot. The truth turned out to be weak van der Waals forces imparted by a multi-length scale

system of hairs that generate incredible amounts of adhesive forces in a tiny area.<sup>7-8</sup> Since then, many approaches towards mimicking the adhesion imparted by this system for synthetic materials have been investigated.<sup>9-10</sup>

All of these properties, and many others found in nature, are desirable for human engineers to create synthetic materials that mimic these properties. The biology inspired field of material design has produced many unique, functional materials.<sup>11</sup> The applications of these materials span all topics. Recently, a bioinspired extracellular matrix was reported that significantly increases renal tissue regeneration.<sup>12</sup> A green synthesis route to generate advanced carbon nanocomposites drawing inspiration from mussel tissues was also recently published.<sup>13</sup> In another composite application, colloidal ‘platelets’ were synthesized and implemented in a polymer matrix, allowing for the combination of high tensile strength and high ductility, usually two properties in opposition.<sup>14</sup> All of these materials provide examples of advances towards the material engineering field that use biomimetic principles to solve the engineering challenge.

While many advances have been made, the material selection used is spread out. With the current synthetic toolbox that chemists and engineers have, it may be advantageous to narrow down the types of chemistries and materials used to generate next-generation advanced biomimetic materials. Looking towards nature for inspiration, all of the natural materials mentioned are made from one type of material: peptides. The exact control of length, sequence, and stereochemistry in peptides, proteins, and enzymes impart the beautiful and ingenious function that these biomacromolecules have. In addition, our understanding of polypeptides is constantly growing. While the fundamentals are now being taught in introductory biochemistry

textbooks,<sup>15</sup> sophisticated models are being generated that are allowing for *de novo* design and prediction of peptide assemblies.<sup>16</sup> In addition, directed evolution has generated another method to generate nature inspired and built materials with specific functionality desired by engineers.<sup>17-18</sup> The continued growth in the understanding of engineering polypeptides positions such a material as the perfect fit for starting to rationally design biomimetic materials.

## **1.2 The Coiled-Coil Peptide Motif**

The sequence, length, and stereochemical control that polypeptide offer allow for seemingly endless design motifs to use in materials. The common  $\alpha$ -helix and  $\beta$ -sheet secondary structures generate a variety of tertiary structures. One that may be of interest in material design is the coiled-coil peptide motif. This motif is characterized by a relatively short peptide sequence, and a self-assembly behavior driven by hiding the hydrophobic residues on the inside of the assembly; its *de novo* design has recently been reported.<sup>19</sup>

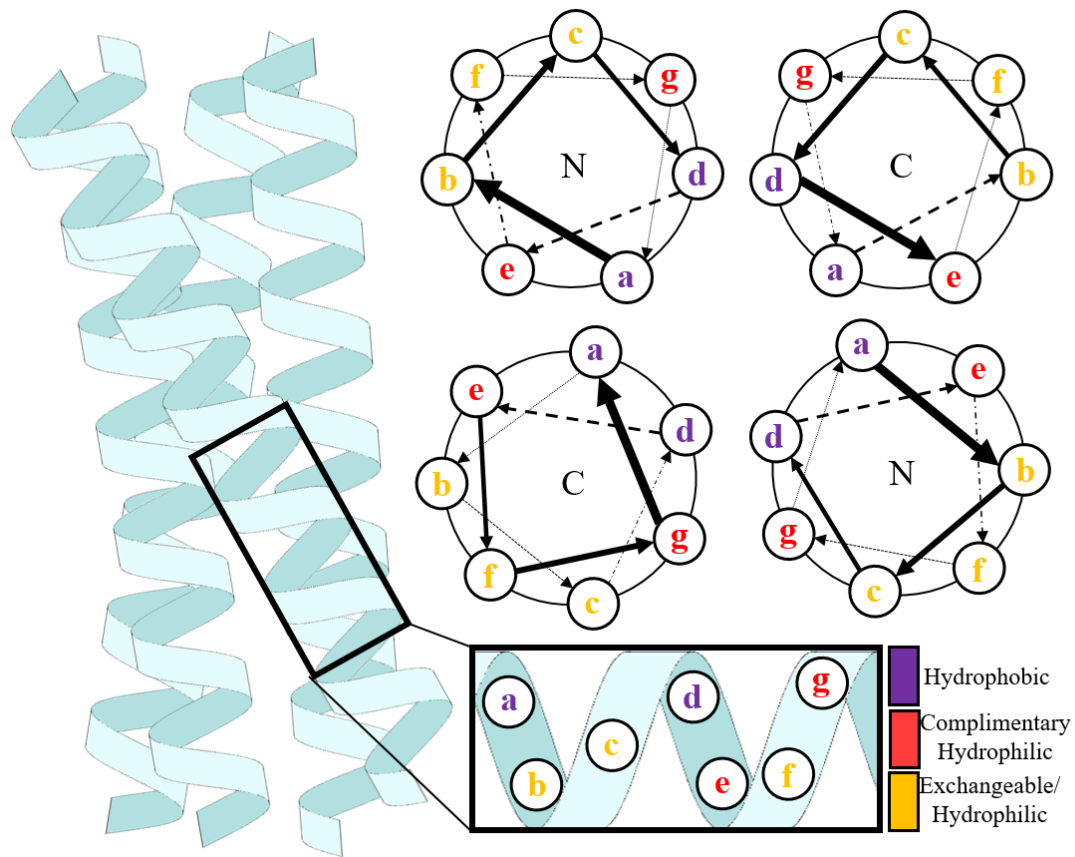


Figure 1 A version of the coiled-coil peptide motif showing an anti-parallel homotetrameric collection of  $\alpha$ -helices. The peptide sequence is characterized by the heptadic repeat unit  $abcdefg$ . The amino acids  $a$  and  $d$  are hydrophobic and are hidden towards the inner core of the assembly. Amino acids  $e$  and  $g$  are hydrophilic in nature and provide complimentary interactions that stabilize the assembly. The amino acids  $b$ ,  $c$ , and  $f$  are often exchangeable and are not important in the assembly of this peptide motif. C and N denote the carbon and nitrogen termini of the peptides.

This self-assembly has a temperature, and to a lesser extent, pH dependence, imparting dynamic control from the beginning. Perhaps the most appealing aspect of this peptide motif is its assembly's robustness against sequence change. While the

inner hydrophobic core is imperative, the hydrophilic moieties on the outside of the assembly can be altered without impacting the assembly's structural integrity. Therefore, engineered sequence changes can be used to design a peptide that function as a material.

In addition to the natural advantages that this peptide motif provides, the *de novo* design, which allows for peptides not appearing in nature, combines the power of nature's chemistry with engineering design principles to generate sequences for any application. With further development, the coiled-coil peptide motif could become the building-block for any structural or dynamic macromolecular material, as the peptide has become the building block for the natural world's materials.

### **1.3 Solid-State Peptide Synthesis**

Recombinant methods in various biological systems have been established for designer peptide and protein expression.<sup>20-21</sup> Recently, non-canonical amino acids are starting to be encoded in DNA to generate peptide sequences that are not realizable in nature.<sup>22</sup> While these methods are robust and essential to current biochemical engineering research, they require special techniques and are not necessary for all applications. If the sequence is short enough, generating the sequences synthetically is advantageous. There have been various protection chemistries developed to impart the sequence defined control that biological enzymes offer. The most popular chemistry is Fmoc protection chemistry. This synthetic route grows polypeptides one residue at a time, coupling the exposed amine on a polypeptide to the carboxylic acid of the amino acid that is being added. The amine of the new amino acid is protected with a fluorenylmethyloxycarbonyl (Fmoc) protecting group, which prevents undesirable reactions. Then the Fmoc group is removed using piperidine, and the next amino acid

is added. The growing polypeptide is grown on a solid-support, usually a porous polystyrene material.<sup>23</sup> Figure 2 below shows the iterative approach to polypeptide synthesis using Fmoc protection.

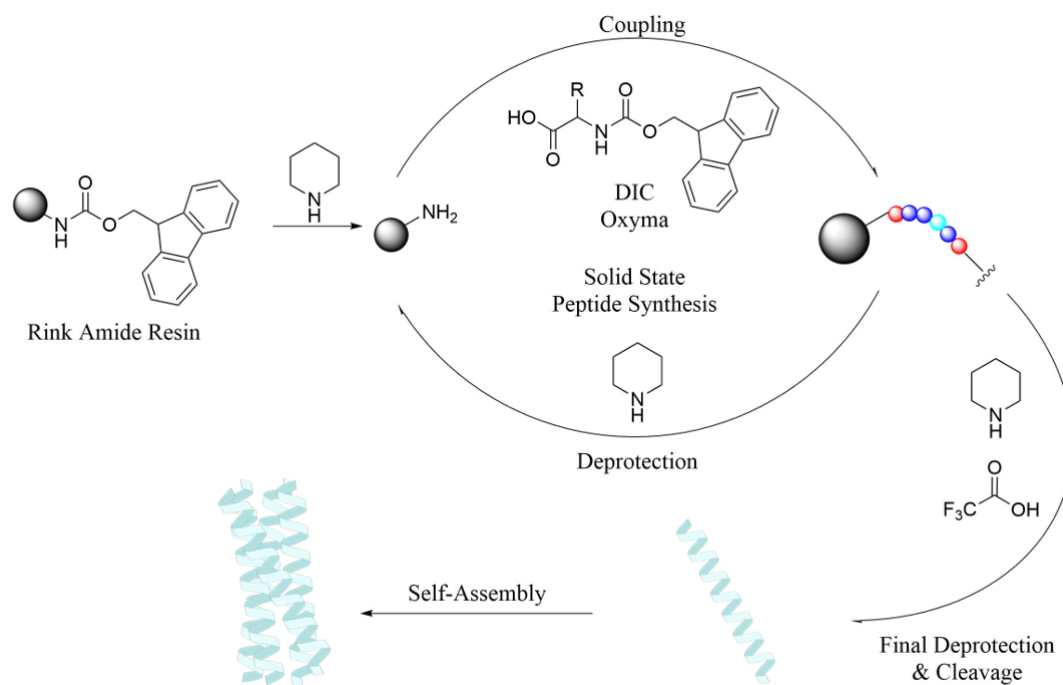


Figure 2 The iterative approach to generating polypeptides on a solid-state support. An amine functionalized resin reacts with a amine-protected amino acid, generating the first residue in the sequence. Then, piperidine removes the Fmoc group to reveal an amine that can react to the next protected amino acid. The final polypeptide design is then cleaved from the solid support using trifluoroacetic acid.

This synthetic process has become more robust due to the implementation of microwave technology. The addition of microwaves into the reaction vessel during amide bond formation reduces reaction times, reduces side reactions, increases yields,

and increases reproducibility of synthesis.<sup>24</sup> With current automation, thirty repeat unit polypeptides can be synthesized in a matter of hours with sequence control and usable yields.

Solid-state microwave-assisted peptide synthesis allows for the efficient and expedient synthesis of non-natural peptides. Overall, this technique allows for peptides to be a convenient base material for material design and synthesis. This synthetic method will be used to generate the basis for materials designed in this work.

#### **1.4 Macromolecular Design Chemistries**

Synthetic macromolecules are a recent scientific invention and primitive when compared to biomacromolecules; only recently, scientists have started to generate chemistries that approach the design control that nature has. Two broad classes of chemistries have recently been developed that are starting to allow for precise macromolecular design: controlled radical polymerization and click chemistry.

The underlying issue that controlled radical polymerization addresses is that polymerizations are hard to control.<sup>25</sup> Especially in radical chain-growth polymerizations, where one monomer is added on to a growing chain, synthetic chemists struggled with generating macromolecules that were similar to biomacromolecules (i.e. macromolecules that have identical length, sequence, etc.). The underlying issues were that the polymerizations had no ‘engineering’ control; the design equations were based on the realities of the natural polymerization. The concept of controlled radical polymerizations (CRP) was to add something to the reaction that would slow and control the polymerization, so that a specific uniform length was reached. Two famous CRPs are atom transfer radical polymerization (ATRP) and reversible addition-fragmentation chain-transfer polymerization (RAFT).

ATRP was pioneered in Dr. Krzysztof Matyjaszewski at Carnegie Mellon University, and has since developed into one of the premier polymer chemistries utilized in materials engineering.<sup>26</sup> ATRP works by reversibly activating and deactivating the reactive site of the growing polymer chain; this reversible activation accomplished by the incorporation of copper halogen salts. The mechanism of polymerization that is currently accepted is displayed below in Figure 3. ATRP tolerates various solvents, halogens, ligands, and monomers; various geometries such as brush and star polymers are easily realizable with ATRP chemistries.

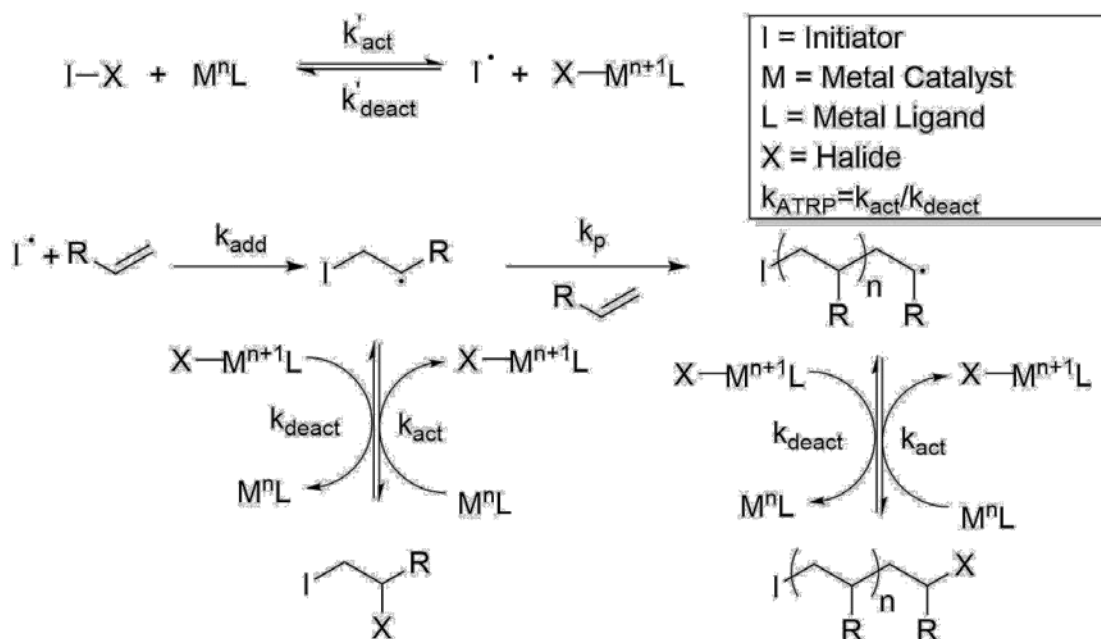


Figure 3 The mechanism for polymer synthesis via atom transfer radical polymerization. When an initiator is initiated, a primary vinyl monomer is added via normal radical polymerization. The growing radical can either add another monomer, or deactivate via the addition of a halogen adduct. Once deactivated, the growing chain will not add another monomer until it is activated, in which case it can proceed to add another monomer via a radical addition. The equilibrium defined by the activation and deactivation controls the kinetics of the polymerization.

The usefulness of ATRP chemistries allows for impactful applications, including precise nanostructuring of materials and advanced biomedical applications.<sup>27-28</sup> For example, ATRP synthesized amphiphilic polyplexes were synthesized for the design of drug-carrying micelles for novel drug release applications.<sup>29</sup> In addition, monomers containing saccharide, peptide, and nucleobase functionalities have been successfully polymerized with ATRP, allowing for novel bioinspired materials.<sup>27</sup>

ATRP allows polymer chemists to generate low dispersity polymers at targeted lengths. This plays the role of, for example, DNA polymerase in generating nature's code. There is still a need for the ability to attach macromolecules together with exact chemoselectivity. For example, inteins are sophisticated natural protein technologies that attach two large peptide blocks at a specific point.<sup>30</sup>

The synthetic solution to exact conjugations is click chemistry. Click chemistry, described in Dr. K. Barry Sharpless' seminal work, is a set of chemical reactions that proceed to quantitative yield under mild conditions, with minimal and harmless byproducts.<sup>31</sup> Conveniently, many of these click reactions are biorthogonal and can be implemented into biological or bioinspired systems with exquisite control.<sup>32</sup> Recently, these reactions are starting to become important chemistries for materials design.<sup>33</sup> Due to their inherent nature, this set of chemical reactions allows for the precise linking of various macromolecules. Both CRP and click chemistry are now instrumental techniques in material synthesis and design. They allow for unprecedented synthetic control of macromolecules, affording the synthesis of materials with precisely defined structures.

## **1.5 Dynamic Hydrogels**

Hydrogels in general are defined as a cross-linked polymeric network that is swelled with water molecules. This class of materials is one of the most studied, generating many biomedical applications, due to its biological compatibility.<sup>34</sup> One of the more promising versions of hydrogels are dynamic hydrogels. These are materials that respond to a stimulus or to stimuli in a controlled manner, such as degradation or controlled release.<sup>35-36</sup> The stimuli vary in type and application, ranging from temperature to light. The advantage of such a material is that the dynamic behavior starts to mimic functionality seen in nature. For example, it is well documented that bone strengthens itself when loaded with stress.<sup>37</sup> These sorts of dynamic behaviors, when realizable, will allow for the design of materials that truly mimic nature.

## **1.6 Thesis Overview**

The goal of the work presented is to investigate different macromolecular geometries attainable from *de novo* designed coiled-coil motifs. Specifically, novel geometries that are not readily available via other material systems are investigated. The synthesis of these geometries are probed using the combination of solid-state microwave-supported peptide synthesis with the macromolecular design chemistries elaborated on in the introduction to this work. In chapter two, work towards generating a macromolecular sphere is presented. In general, such a geometry can provide a platform to study macromolecular physics as well as self-assembly behavior and driving forces of peptide materials. In chapter three, the synthesis of star polymer-peptide conjugates is shown; grafting-from techniques to generate the conjugates are presented. This geometry represents a macromolecule that can provide dynamic behavior in materials to various stimuli. In chapter four, conclusions to this work are

presented, along with concepts about future studies that these novel geometries are suited for.

## Chapter 2

### COVALENT STABILIZATION OF THE COILED-COIL MOTIF

#### 2.1 Introduction

Polypeptide assemblies are inherently designed for biological conditions i.e. biologically relevant solvent, temperature, pH, etc. In many material applications, however, it is necessary for materials to perform their desired functionality in different environments. Therefore, in order to utilize the coiled-coil motif in many applications, it is desirable to permanently generate the self-assembly. While the assembly is driven by secondary interactions, covalent stabilization is an attractive method to permanently lock the structure in place. A common example is found in nature; disulfide bridges covalently lock in tertiary and quaternary structures.<sup>15</sup>

In Figure 4 below, the proposed covalent stabilization schematic for a homotetrameric coiled-coil bundle is shown. Small molecule choice and peptide sequence is essential. Note that the stabilization will happen post-assembly, and therefore the reaction chemistry used needs to be tolerable to aqueous conditions.

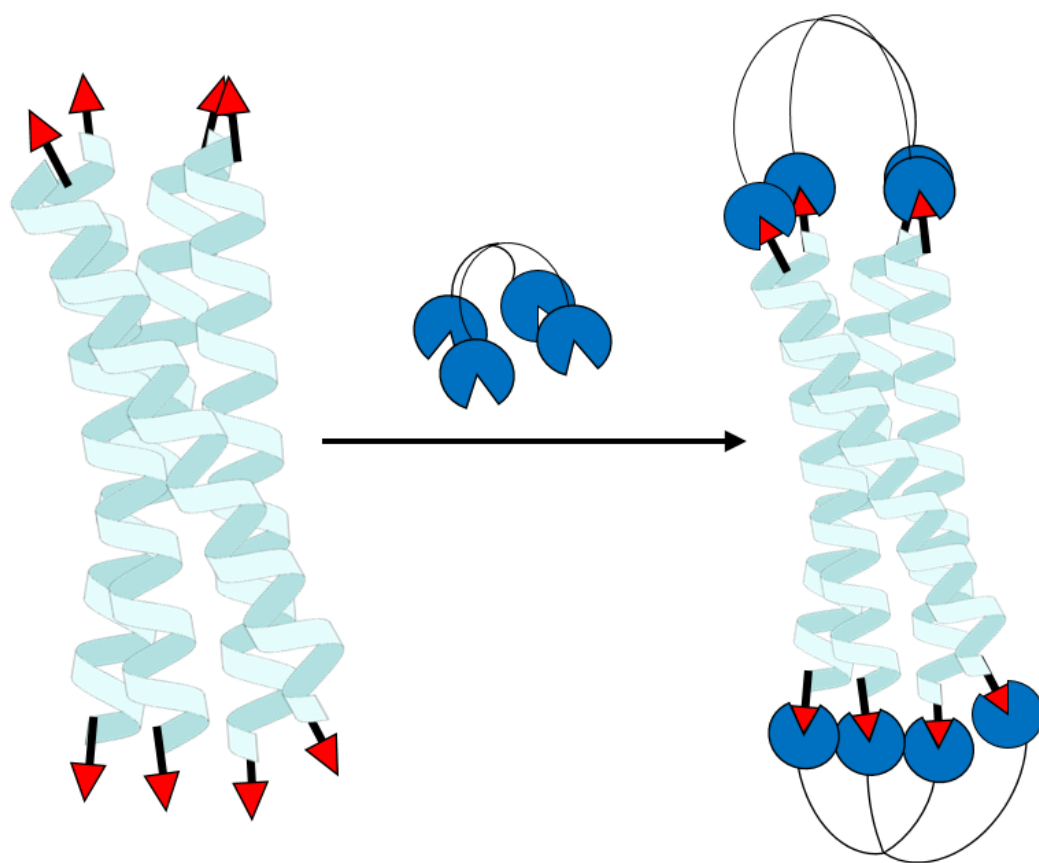


Figure 4 Schematic showing the covalent stabilization hypothesized. A peptide functionalized on both termini with a special chemical moiety self assembles to form a coiled-coil bundle with four reactive handles on the top and bottom of the assembly. A tetra-functionalized small molecule can react to the peptide to covalently lock the assembly architecture.

In order to produce covalent stabilization, the chemistry involved needs to be highly efficient and chemoselective; for this, click chemistry offers a solution. The copper(I)-catalyzed alkyne-azide cycloaddition (CuAAC) offers these properties, and is conveniently biorthogonal, so it will not interact with the natural chemical residues present in the peptides. Amino acids containing azides have been reported and allow

for the synthesis of peptides with CuAAC functionality. In combination with small molecule alkynes, attempts at covalent stabilization of these coiled-coil bundles are presented.

## 2.2 Materials and Experimental Methods

### 2.2.1 Monomer Synthesis

The synthesis of the tetraalkyne 3-(3-(prop-2-yn-1-yloxy)-2,2-bis((prop-2-yn-1-yloxy)methyl)propoxy)prop-1-yne was conducted following a procedure described elsewhere.<sup>38</sup> Into a round bottom flask connected with a reflux condenser under nitrogen purge, pentaerythritol (10 g, 73.45 mmol), potassium hydroxide (57 g, 1016 mmol), and tetrabutylammonium iodide (0.35 g, 0.95 mmol) in 250 ml of tetrahydrofuran were added. Then, propargyl bromide (65.45 ml of 80% solution in toluene, 691 mmol) was added dropwise into the reaction vessel, followed by heating the reaction mixture to 70 °C. The reaction mixture was agitated for 3.5 hours. The reaction mixture was extracted with ethyl acetate, water, and 1 M sodium hydroxide, and dried with magnesium sulfate. The product was recrystallized in ethyl acetate at 4 °C as a pale brown crystal. The chemical structure and corresponding NMR can be found in Appendix B.

### 2.2.2 Peptide Synthesis

Peptides were prepared at a 0.10-mmol scale on a Rink amide resin using a Liberty Blue peptide synthesizer. Standard Fmoc-based protocols were used. First, the base labile Fmoc group is cleaved using 20% piperidine in DMF to deprotect the amine, followed by washing steps and coupling of the next amino acid in the sequence using DIC and oxyma pure. The synthesizer uses a microwave to achieve elevated

temperatures to minimize reaction times and dramatically cuts down the overall time required for synthesis. Iterations are repeated until the desired length and sequence of the peptide is achieved. To cleave the peptide from the resin, the resin was agitated for two hours in a cleavage solution comprised of (by volume) 95% trifluoroacetic acid, 2.5% triisopropylsilane, 2.5% Milli-Q water, and 50 mg/mL phenol. The peptide was precipitated dropwise into diethyl ether to facilitate it solidifying. The mixture was centrifuged, and the supernatant was discarded. This process precipitation process was repeated two more times, and the resultant crude peptide was dried under nitrogen.

For the addition of azides onto the peptide, alloc-protected lysines were incorporated in the beginning and end of the peptide sequence. The terminal amine was capped with an acetate group using a 90:5:5 (v:v) DMF:N,N-Diisopropylethylamine:Acetic Anhydride reaction solution. Then, the lysines were deprotected using a Palladium catalyst. Finally, an amide coupling reaction was performed using azido-butyric acid with 2-(1*H*-benzotriazol-1-yl)-1,1,3,3-tetramethyluronium (HBTU) as the coupling reagent. Once the azide was attached, the peptide was cleaved following the procedure outlined above. Reaction conditions for these reactions were modified from procedures in Hermansen.<sup>23</sup>

### 2.2.3 Peptide Purification

Purification was performed via reverse-phase high-performance liquid chromatography (HPLC). Prior to HPLC injection, crude peptide was dissolved in 95%(v/v) Milli-Q water and 5%(v/v) acetonitrile, each containing 0.1% (by volume) trifluoroacetic acid and was filtered with 0.45- $\mu$ m filters. The products were subjected to an elution gradient of 70% solvent A [0.1% (by volume) trifluoroacetic acid] to 50% solvent A in 20 minutes; solvent B was acetonitrile with 0.1% (by volume)

trifluoroacetic acid. Fractions were collected by monitoring the absorption of ultraviolet-visible light at 214 nm. Collected fractions are analyzed by mass spectroscopy. Pure fractions were combined and lyophilized to produce pure peptide product.

#### 2.2.4 Conjugation Conditions

Conjugation reactions were performed in 30% dioxane in water solutions in order to solubilize the tetraalkyne. In a typical reaction, copper sulfate (1 eq.), sodium ascorbate (4 eq.), and tris-hydroxypropyltriazolylmethylamine (THPTA) as a ligand (2 eq.) were added to a 2 mM solution of the diazide peptide. Then 2 equivalents of the tetraalkyne were added into the reaction solution and the reaction was allowed to proceed at room temperature overnight. Conjugation was tracked by mass spectroscopy.

#### 2.2.5 Characterization

##### A. Nuclear Magnetic Resonance (NMR) Spectroscopy

NMR spectra were obtained from a Bruker AV 400 NMR Spectrometer. All samples for obtaining the  $^1\text{H}$  NMR spectrum were prepared in deuterated chloroform.

##### B. Circular Dichroic Spectroscopy

Circular Dichroic spectroscopy was performed on a Jasco J-1500 Circular Dichroism Spectrophotometer. All samples were run at 0.1 mM in water unless otherwise noted.

##### C. Mass Spectroscopy

Mass spectroscopy was conducted using a Waters Acquity H-Class UPLC for LC-MS with an ESI source. A 2.5 minute run time is used.

### **2.3 Results and Discussion**

The chemistry used for this study was the CuAAC reaction. Deciding whether to add alkynes or azides to the peptide was driven by safety. Low molecular weight azides are known to be explosive and the synthesis of such is avoided. Therefore, the peptide was functionalized with azide and the small molecule to stabilize the assembly was a multi-functional alkyne. The small molecule synthesized was chosen due to its prevalence in the literature, as well as its size.<sup>38</sup> The small arms of the linker were hypothesized to maximize the chances of reacting only to the azides of the same assembly, avoiding cross conjugation. The <sup>1</sup>H NMR of the tetraalkyne is in Appendix B. The peptide sequence used was a modification of a known sequence in literature.<sup>19</sup> The mass of the new peptide was confirmed via mass spectroscopy, and to confirm the self-assembly of the novel peptide, CD spectroscopy of the peptide in solution was conducted, as shown below in Figure 5.

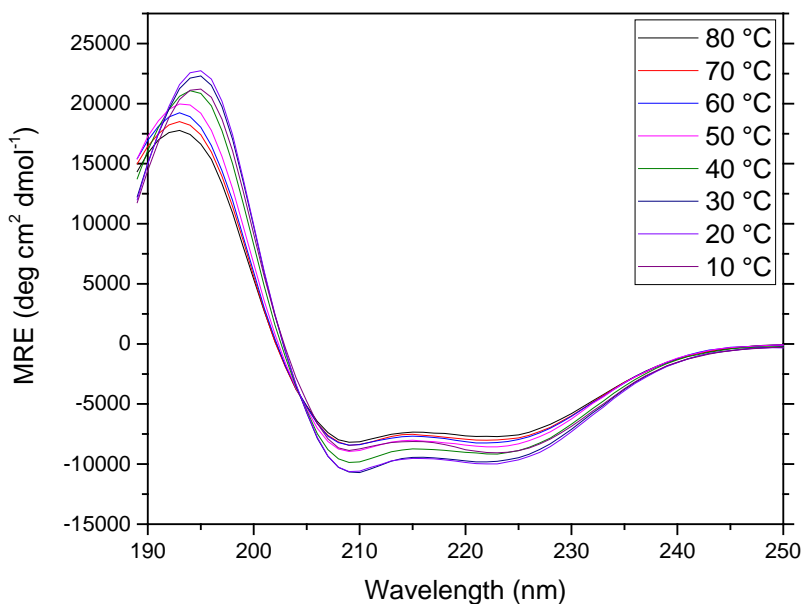


Figure 5 CD spectrum of the diazide peptide. The typical minima at 208 nm and 222 nm are indicative of the assembly of the diazide peptides into coiled-coil bundles.

Once the self-assembly of the functionalized peptide was confirmed, the subsequent conjugation was considered. The most important part of this conjugation is finding conditions that do not create dimers, trimers, or polymerize the bundles. At high concentrations of peptide, the coiled-coils may link to each other via the small molecule bridge. In order to avoid this, as mentioned above, the monomer synthesized has small arms, allowing it to react with azides that are close by. In addition, the concentration of peptide in solution was kept low in order to force the azide functionalities to all react with the same tetraalkyne. If successful, the stabilized peptide could be confirmed by a mass increment in the mass spectroscopy measurement. Unfortunately, the new mass did not correlate to the addition of two

tetraalkynes; cross-conjugations were occurring. While different reaction conditions were attempted, no successful covalent stabilization was achieved. See Appendix B for conjugation details.

## **2.4 Summary and Conclusions**

A diazide peptide was prepared that self-assembled into the coiled-coil motif with four functional handles on the top and the bottom of the assembly. A tetraalkyne small molecule was synthesized in order to conduct the CuAAC reaction to covalently stabilize the peptide assembly. No successful conjugations were observed, as it was hard to control which peptides the small molecule conjugated to. In order to successfully achieve this geometrical stapling, a secondary interaction template may be required to ensure the small molecule only reacts with one of the assemblies. Alternatively, other covalent stabilizations can be pursued. Specific functionalities can be placed in the side of the peptide, allowing for the stapling of peptides on the side of the assembly. In addition, an assembly where there are two functionalities on the top and bottom may allow for the successful stabilization, with more flexibility and freedom of the resultant macromolecular geometry.

## Chapter 3

# SYNTHESIS OF POLYMER-PEPTIDE CONJUGATES WITH STAR GEOMETRIES

### 3.1 Introduction

Polymer-peptide conjugates are a growing class of materials that combine the benefits of synthetic polymer chemistry and biological peptide chemistry in a hybrid material with many target applications. These conjugates have been gaining attention in recent years due to their improved performance over purely biological or purely synthetic systems in certain applications. For example, researchers have shown the ability to rationally tune the enzymatic activity by controlling the extent of polymer grafting.<sup>39</sup> In addition, this class of materials has shown advantages in self-assembly and therapeutics delivery.<sup>40-41</sup>

In general, the two methods to produce these conjugates are grafting-to and grafting-from. In grafting-to, polymers are covalently attached to polypeptides at specific chemical points. A common application of this method is the PEGylation of proteins for increased bioavailability.<sup>42</sup> Note that biorthogonal click reactions are very popular candidates for the chemistries involved in grafting-to conjugates.<sup>23</sup>

Grafting-from synthesizes polymers from the polypeptide, as the name implies. Recently, on resin grafting-from was performed generating well defined hybrid materials with simplified syntheses and purification.<sup>43</sup> For grafting-from to occur, a polymerization initiator needs to be attached onto the biomacromolecule. Then, polymerizations are conducted *in situ* off of the peptide. This method commonly utilizes CRP, as it affords the best control over the polymerization, creating conjugates that are similar in nature. Recently, chymotrypsin was modified with a synthetic polymer via an ATRP grafting-from approach to predictably and rationally tune

enzymatic activity and stability.<sup>39</sup> Clearly, the synthesis of these hybrid materials generate new functionality and control over polypeptides, allowing for advanced materials to be synthesized.

The current homotetrameric coiled-coil bundle that was employed in the covalent stabilization work allows for the generation of a star geometry; single initiator sites on each peptide, when self-assembled, allows for a grafting-from strategy to generate this novel macromolecular geometry.

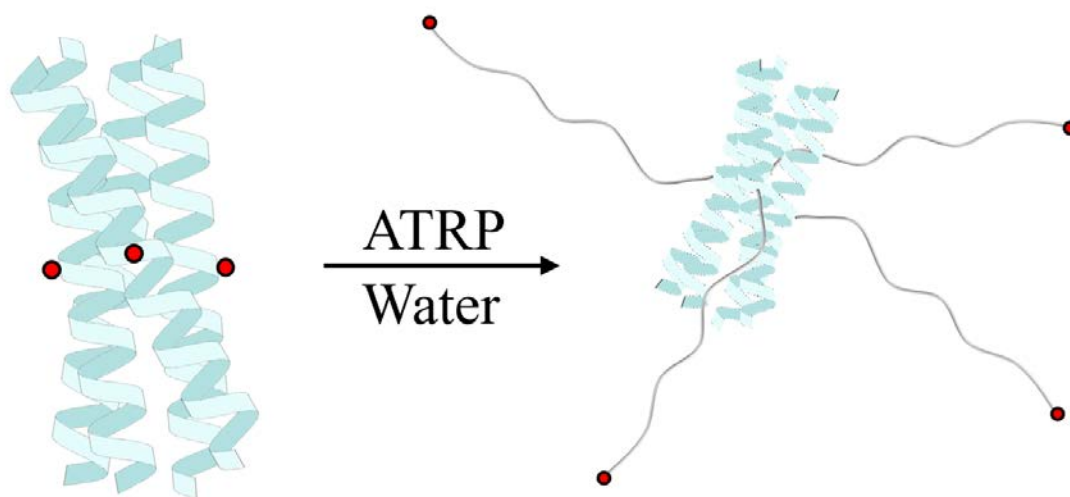


Figure 6 The proposed star geometry polymer-peptide conjugate using aqueous ATRP to control the polymerization of the growing chains off of the peptide. Once generated, this star polymer-peptide conjugate will have a dynamic central linkage that will respond to thermal stimulus.

The polymer arms of the star-shaped conjugate can have solvent, temperature, and pH dependence that affects its physical behavior in solution, as well as its interactions with the peptide assembly. The peptide assembly, having its own dynamic

stimuli, will contribute to the interesting behavior of this hybrid material. This chapter details the work towards realizing this novel geometry with emphasis on the peptide structure and polymerization chemistry.

## **3.2 Materials and Experimental Methods**

### **3.2.1 Peptide Synthesis**

Peptides were prepared at a 0.10-mmol scale on a Rink amide resin using a Liberty Blue peptide synthesizer. Standard Fmoc-based protocols were used. First, the base labile Fmoc group is cleaved using 20% piperidine in DMF to deprotect the amine, followed by washing steps and coupling of the next amino acid in the sequence using DIC and oxyma pure. The synthesizer uses a microwave to achieve elevated temperatures to minimize reaction times and dramatically cuts down the overall time required for synthesis. Iterations are repeated until the desired length and sequence of the peptide is achieved. To cleave the peptide from the resin, the resin was agitated for two hours in a cleavage solution comprised of (by volume) 95% trifluoroacetic acid, 2.5% triisopropylsilane, 2.5% Milli-Q water, and 50 mg/mL phenol. The peptide was precipitated dropwise into diethyl ether to facilitate it solidifying. The mixture was centrifuged, and the supernatant was discarded. This process precipitation process was repeated two more times, and the resultant crude peptide was dried under nitrogen.

For the addition of branched amino acids and initiators onto the peptide, alloc-protected lysines were incorporated in the middle of the peptide sequence. The terminal amine was capped with an acetate group using a 90:5:5 (v:v) DMF:N,N-Diisopropylethylamine:Acetic Anhydride reaction solution. Then, the lysine was deprotected using a Palladium catalyst. For additional branch amino acids, hand

couplings on resin were performed using similar reaction conditions provided above. Finally, an amide coupling reaction was performed using 2-bromo-2-methylpropionyl bromide with trimethylamine in dichloromethane. Once the branched amino acids and the initiator were attached, the peptide was cleaved following the procedure outlined above. Reaction conditions for these reactions were modified from procedures in Hermansen.<sup>23</sup>

### 3.2.2 Monomer Synthesis

The small molecule ATRP initiator was synthesized by modifying a procedure in literature.<sup>39</sup> A mixture of 2-bromo-2-methylpropionyl bromide (40 mmol, 4.92 ml) and dichloromethane (DCM, 20 ml) was slowly added into a solution of glycine (40 mmol, 3 g) and sodium hydrogen carbonate (100 mmol, 8.4 g) in deionized water (80 ml) on an ice bath. The mixture was stirred at room temperature for two hours. The water phase was washed with DCM thrice. The product was extracted with ethyl acetate and the organic phase was dried with magnesium sulfate. The product was purified by recrystallization from a mixture of diethyl ether and n-hexane (1:9 v:v).

### 3.2.3 Peptide Purification

Purification was performed via reverse-phase high-performance liquid chromatography (HPLC). Prior to HPLC injection, crude peptide was dissolved in 95%(v/v) Milli-Q water and 5%(v/v) acetonitrile, each containing 0.1% (by volume) trifluoroacetic acid and was filtered with 0.45- $\mu$ m filters. The products were subjected to an elution gradient of 70% solvent A [0.1% (by volume) trifluoroacetic acid] to 50% solvent A in 20 minutes; solvent B was acetonitrile with 0.1% (by volume)

trifluoroacetic acid. Fractions were collected by monitoring the absorption of ultraviolet-visible light at 214 nm. Collected fractions are analyzed by mass spectroscopy (see chapter 3.2.5). Pure fractions were combined and lyophilized to produce pure peptide product.

### 3.2.4 Grafting-from Polymerization Conditions

The following polymerization is a modified procedure from Murata et al.<sup>39</sup> In a typical reaction, water was degassed using the freeze-pump-thaw method, conducting three iterations of the cycle. A 0.0078 M stock solution of 1:1 copper bromide:HMTETA (1,1,4,7,10,10-hexamethyltriethylenetetramine) was prepared. 2-(Dimethylamino)ethyl methacrylate (DMAEMA) was purified by passing it through a basic alumina plug. Peptide (0.00075 mmol, 2.8 mg) and DMAEMA (0.0246 mmol, 3.9 mg) were added into a 4-dram screw vial with a magnetic agitator and sealed with a rubber septum. Catalytic solution was added to achieve a 5:1 catalyst:initiator ratio. Then, water was added to achieve a peptide concentration of 1.15 mM. The reactions were allowed to proceed for 20 hours.

### 3.2.5 Characterization

#### A. Nuclear Magnetic Resonance Spectroscopy

NMR spectra were obtained from a Bruker AV 400 NMR Spectrometer. All small molecule samples for obtaining the <sup>1</sup>H NMR spectrum were prepared via deuterated chloroform. All polymerization samples for obtaining the <sup>1</sup>H NMR spectrum were prepared in deuterium oxide.

#### B. Circular Dichroic Spectroscopy

Circular Dichroic spectroscopy was performed on a Jasco J-1500 Circular Dichroism Spectrophotometer. All samples were run at 0.1 mM in water unless otherwise noted.

### C. Mass Spectroscopy

Mass spectroscopy was conducted using a Waters Acquity H-Class UPLC for LC-MS with an ESI source. A 2.5 minute run time is used.

### D. Matrix-Assisted Laser Desorption/Ionization Time of Flight Spectroscopy

The matrix used in all experiments was purchased from [INSERT]. To prepare a typical sample, a matrix sample was dissolved in 100  $\mu$ l of 1:1 H<sub>2</sub>O:MeCN with .1% trifluoroacetic acid. After being mixed, 10  $\mu$ l of the matrix solution was added to 1, 2, and 5  $\mu$ l of the reaction mixture. Then, 0.5, 1, and 2  $\mu$ l of the matrix-sample solution was plated onto the MALDI plate and allowed to dry for two hours. Compressed air was used after drying to remove any particles; the samples were then ready for analysis.

The following parameters were used for obtaining MALDI spectra: laser frequency of 60 Hz, linear gain detector of 16000 V, and a sampling rate of 1.00GS/s. Spectra were averaged in triplicates.

## 3.3 Results and Discussion

Before performing grafting-from polymerizations, a suitable macroinitiator needed to be prepared. Looking at Figure 1, the amino acid that would serve as the initiator needed to be on the outside of the assembly, which is convenient since those amino acids are exchangeable. The first generation of macroinitiator used a lysine to

attach on an ATRP initiator. Figure 7 below shows the synthetic scheme to generate a macroinitiator.

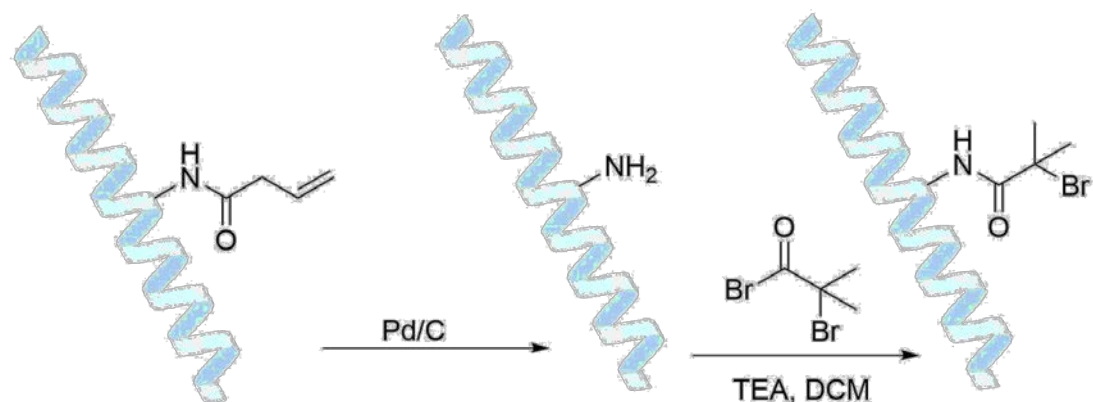


Figure 7 The synthetic route to obtain an ATRP-macroinitiator. Alloc-group deprotection of a centrally located lysine is performed, generating a free lysine that is able to subsequently react. The amide bond formed generates an ATRP-macroinitiator. When self-assembled, each bundle should have four initiating units, all on the outside of the assembly.

Two base sequences with different assembly behavior were used in the synthesis; initially, it was not understood how attaching an ATRP initiator group to the middle of the peptide would affect the self-assembly. The peptides 4459-a-Br and p622-Br, modified from the parent peptide sequences, showed interesting changes in the assembly behavior. In Figure 8 below, the CD of the macroinitiators are displayed.

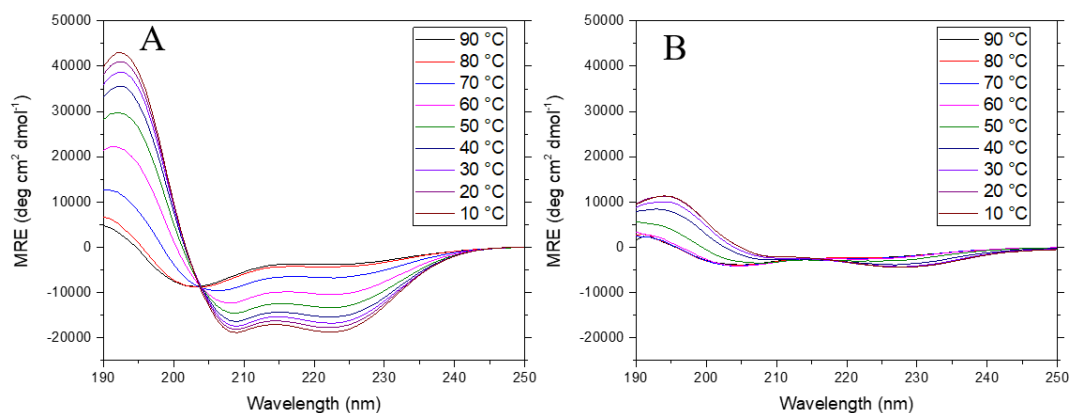


Figure 8 Circular Dichroic spectra of A) 4459-a-Br and B) p622-Br. P622-Br does not assembly into coiled-coil bundles. The 4459-a-Br assemblies like its parent peptide, but its melting behavior shows that it is less thermodynamically stable.

The modification of p622 showed significant changes in the self-assembly behavior, possibly due to the flexible lysine initiator group destructively interfering with the core of the assembly. The 4459-a-Br sequence showed promising assembly, although it begins to melt at a low temperature. From this data, 4459-a-Br was determined to be a successful candidate for the grafting-from synthesis of the conjugates.

A small molecule was synthesized as a platform to test ATRP reaction conditions. To obtain the same electronic properties that the macroinitiator would have, the ATRP initiator was reacted to the amine of a glycine; this small molecule was synthesized by Bryan Sutherland. See Appendix C for the structure and corresponding NMR of the small molecule initiator. Using this small molecule, many different reaction conditions were tested. Table 1 below summarize the reaction conditions used.

Table 1 Reaction tables detailing ATRP conditions for synthesis of star polymer-peptide conjugates. Typical procedure details are described in chapter 3.2.4. Unless otherwise specified, the initiator is the small molecule ATRP initiator, and the solvent is D<sub>2</sub>O.

Reaction	Initiator	Monomer	Copper	Ligand	Solvent	Notes
R <sub>95-1</sub>	1	21	5	5	10 ml	
R <sub>95-2</sub>	1	21	5	5	3 ml	
R <sub>95-3</sub>	1	83	5	5	3 ml	
R <sub>95-4</sub>	1	163	5	5	3 ml	
R <sub>98-1</sub>	1	21	5	5	3 ml	
R <sub>98-2</sub>	0	21	5	5	3 ml	Control showed no polymerization.
R <sub>98-3</sub>	1	21	5	5	1.13 ml	
R <sub>100-1</sub>	1	21	5	5	1.13 ml	
R <sub>100-2</sub>	1	21	5	5	1.13 ml	Freeze-pump-thaw
R <sub>100-3</sub>	1 (4459-a-Br)	21	5	5	1.13 ml	
R <sub>100-4</sub>	1 (4459-a-Br)	21	5	5	1.13 ml	Freeze-pump-thaw (R <sub>102</sub> and onwards uses this degassing procedure.
R <sub>102-1</sub>	1 (4459-a-Br)	33	5	5	650 ul	
R <sub>102-2</sub>	1 (4459-a-Br)	60	5	5	650 ul	
R <sub>102-3</sub>	1 (4459-a-Br)	85	5	5	650 ul	
R <sub>104-1</sub>	1 (4459-a-EBr)	90	5	5	650 ul	
R <sub>104-2</sub>	1 (4459-a-EGBr)	90	5	5	650 ul	
R <sub>104-3</sub>	1 (4459-a-EGEBr)	90	5	5	650 ul	

R <sub>106-2</sub>	1	94	5	5	1.13 ml	
R <sub>106-4</sub>	1	94	5	5 (BiPy)	1.13 ml	
R <sub>106-5</sub>	1	94	5	5 (PMDETA)	1.13 ml	
R <sub>106-6</sub>	1	94	5	5	1.13 ml	50 mM NaBr

The first set of reactions, R<sub>95</sub>, was following a procedure in literature that used a similar macroinitiator to polymerize a monomer, 2-(Dimethylamino)ethyl methacrylate (DMAEMA), via ATRP that has a lower critical collusion temperature (LCST), potentially adding more dynamic behavior to the protein.<sup>39</sup> When analyzed via NMR, high conversions were achieved. The NMR spectrum below shows a representative spectrum of the resultant polymer.

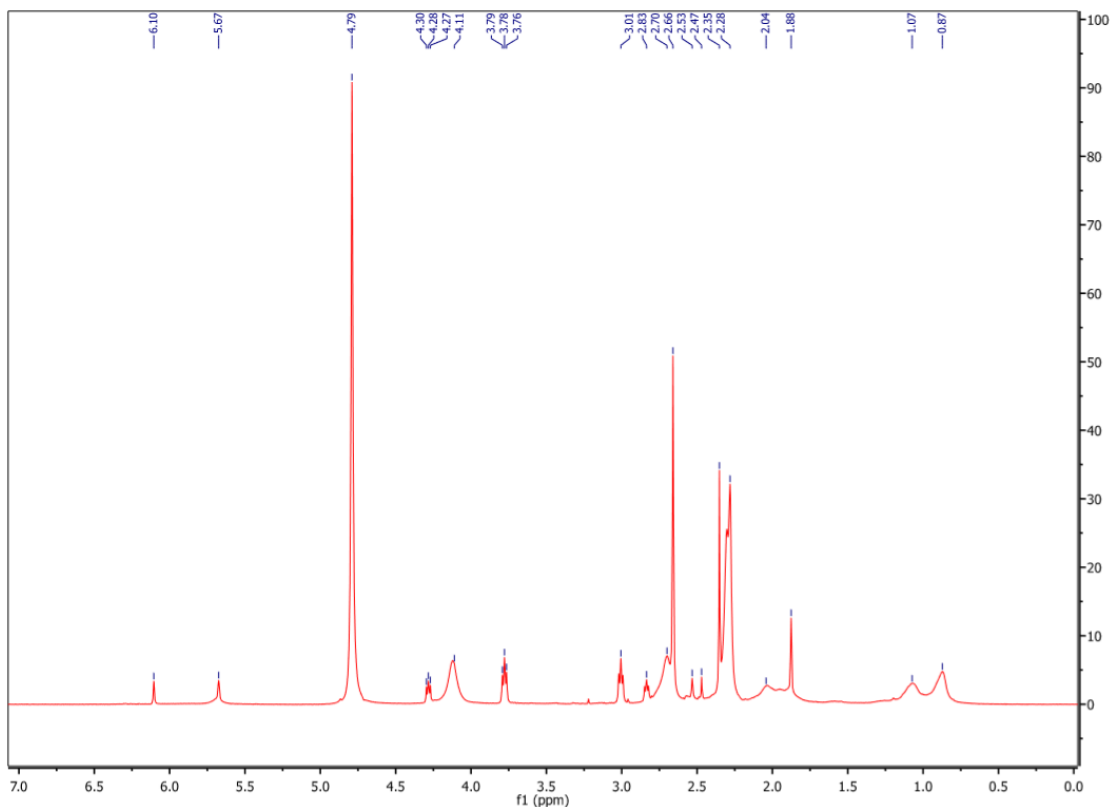


Figure 9 The NMR spectrum of R<sub>95</sub>-2. Peaks at 5.67 and 6.10 ppm are protons of the double bond of the monomer. Peaks at 1.07 and 0.87 ppm are methyl protons generated during the polymerization.

However, this set of reaction had two main problems. The amount of initiator required would not be translatable to the macroinitiator system, due to the limits in the amounts of peptide that can be made on relevant time scales. In addition, the copper amount used was not fully dissolved at the start of the reaction. Changes in the relative and absolute amounts were needed to have a consistent polymerization protocol. In the second set of reactions, R<sub>98</sub>, R<sub>98</sub>-1 was used as a reference of performance from the first reaction. R<sub>98</sub>-2 was setup without the bromide initiator as a control to ensure the polymerization was proceeding via ATRP. R<sub>98</sub>-3 was conducted at a lower

concentration of initiator, decreasing the absolute amount of initiator and copper. NMR spectrum show polymerizations for R<sub>98</sub>-1 and R<sub>98</sub>-3, not R<sub>98</sub>-2, which was promising evidence towards the polymerization proceeding *via* ATRP. To get an accurate measure of the size of the polymer, MALDI spectra was collected. The target molecular weight of R<sub>98</sub>-3 was 3500 Da. The MALDI spectrum below shows a distribution typical of polymers with a mass centered around the target molecular weight.

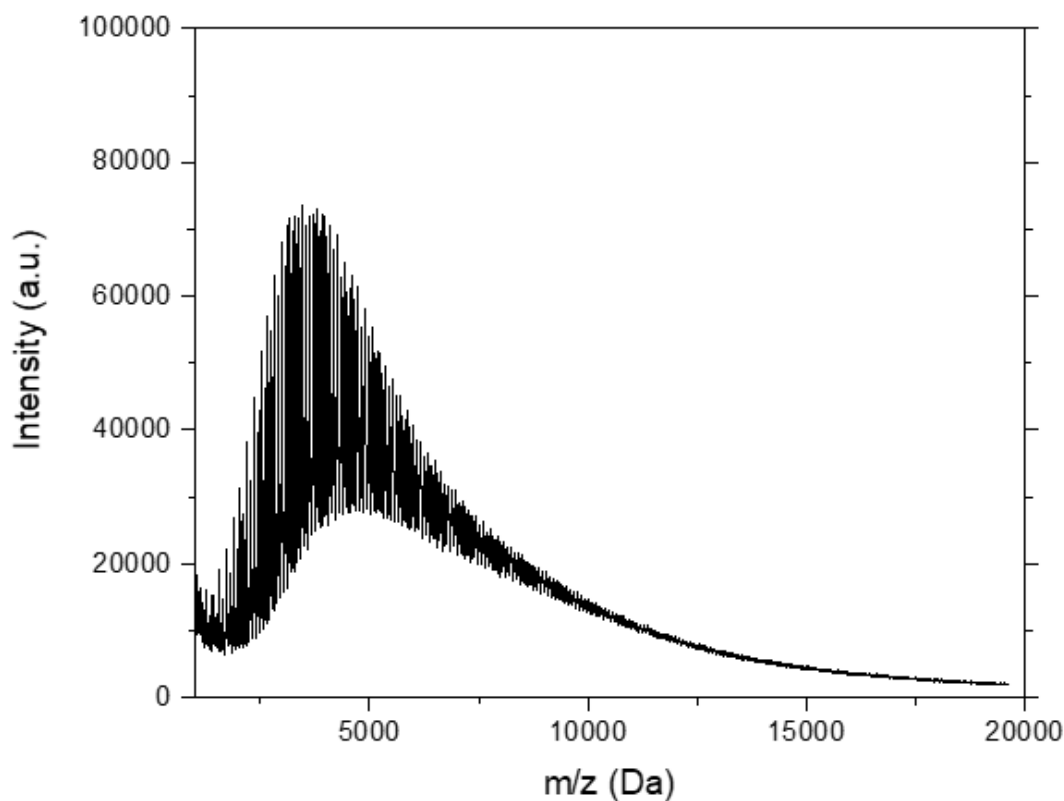


Figure 10 The MALDI spectrum for R<sub>98</sub>-3.

After the successful synthesis and characterization of p(DMAEMA), the R<sub>100</sub> set of reactions tested deoxygenation conditions; freeze-pump-thaw was shown to be marginally better than sparging with nitrogen *via* NMR, and was therefore used for the remainder of this work. In addition, the reaction conditions were tested using the macroinitiator. Figure 11 below shows the MALDI spectrum of the peptide-polymer conjugate under freeze-pump-thaw conditions.

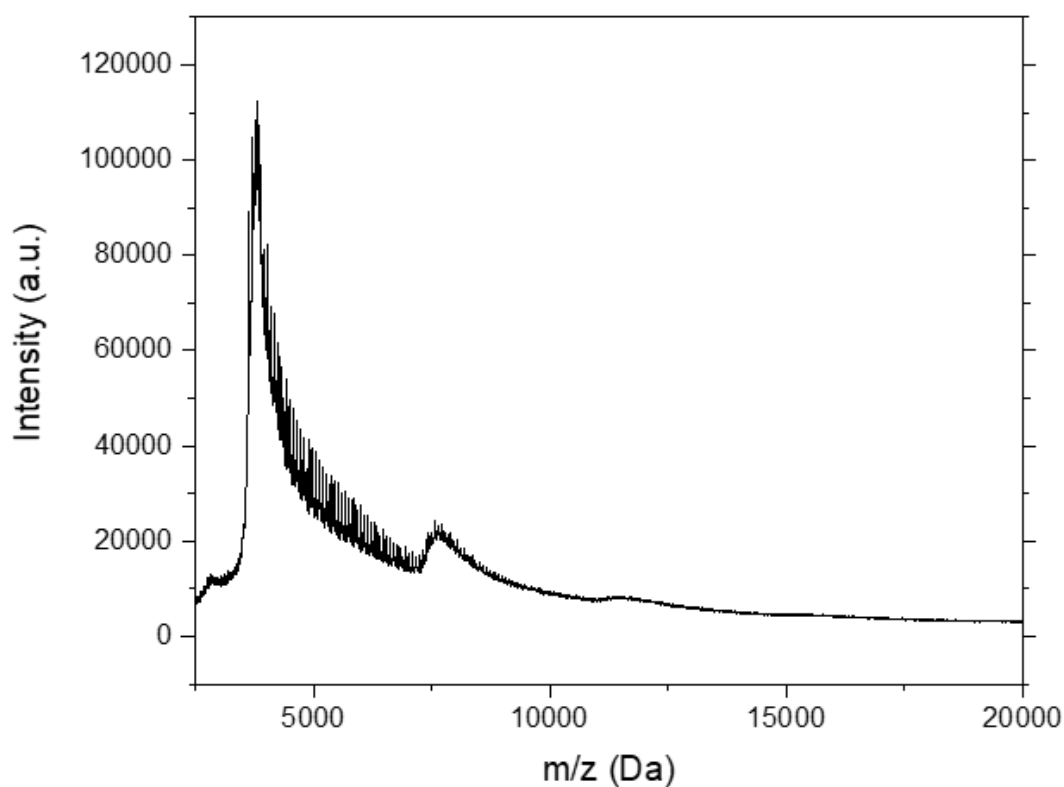


Figure 11 The MALDI spectrum for R<sub>100</sub>-4. Molecular weight of the base macroinitiator is 3753 Da. The peak around 7500 Da is hypothesized to be the +2 charged species of the macroinitiator.

The results show a distribution centered around the initial peptide mass. The desired molecular weight was 7000 Da. The distribution in the MALDI shows the parent peptide population with small amounts of monomer added on, that decreases as the molecular mass increases. The second population at 7500 Da is the plus-2 charge version of the base peptide. This is not the distribution that would show the successful polymerization via ATRP. All peptides should be growing polymer at the same rate, which would be a new peak forming at the target molecular weight with distribution tails before and after. Since the targeted molecular weight is hidden by the spectral artifact, definitive proof of new population formation was not found.

To definitively determine whether the polymer growing off of the peptide is proceeding via ATRP, the R<sub>102</sub> set of reactions targeted different molecular weights that would appear between the n-plus peaks of the base peptide. NMR analysis showed polymerization at smaller conversions, but the broader peaks signaled that a large polymer had formed. In Figure 12 below, the MALDI shows similar behavior to that observed in R<sub>100-4</sub>.

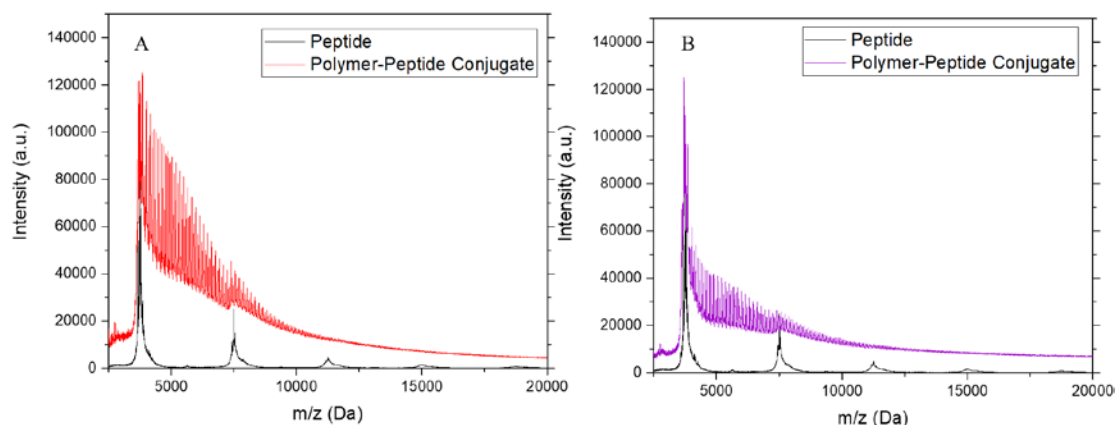


Figure 12 MALDI spectra of A) R<sub>102</sub>-1 and B) R<sub>102</sub>-2, along with the reference peaks of the base peptide. The spectra do not show the formation of a new population centered at the target molecular weight.

The MALDI and NMR data were in disagreement. While NMR showed conversions that would result in high molecular weight conjugates, the MALDI showed small polymers growing off of the base peptide. It is hypothesized that some of the initiators on the coiled-coil bundle are hidden inside the assembly; this is supported by the change in assembly properties of 4459-a-Br. The melting temperature decreased significantly with the addition of the ATRP initiator group, which may be due to the initiator chains hiding in the assembly and destabilizing the structure. If this were true, only a few amount of initiators would use all of the monomer in the system. This would result in high conversion of monomer in the NMR spectra, but the MALDI would not show a high signal of these rare occurrences. To solve this, the initiator chains were extended by adding amino acids to the exposed lysine before attaching the bromide initiator. Extending the initiator away from the assembly may stabilize the structure while making the initiating sites more accessible.

Three different extensions were synthesized by Nicole Halaszynski; the CD spectra of 4459-a-Br and its derivatives are shown below in Figure 13.

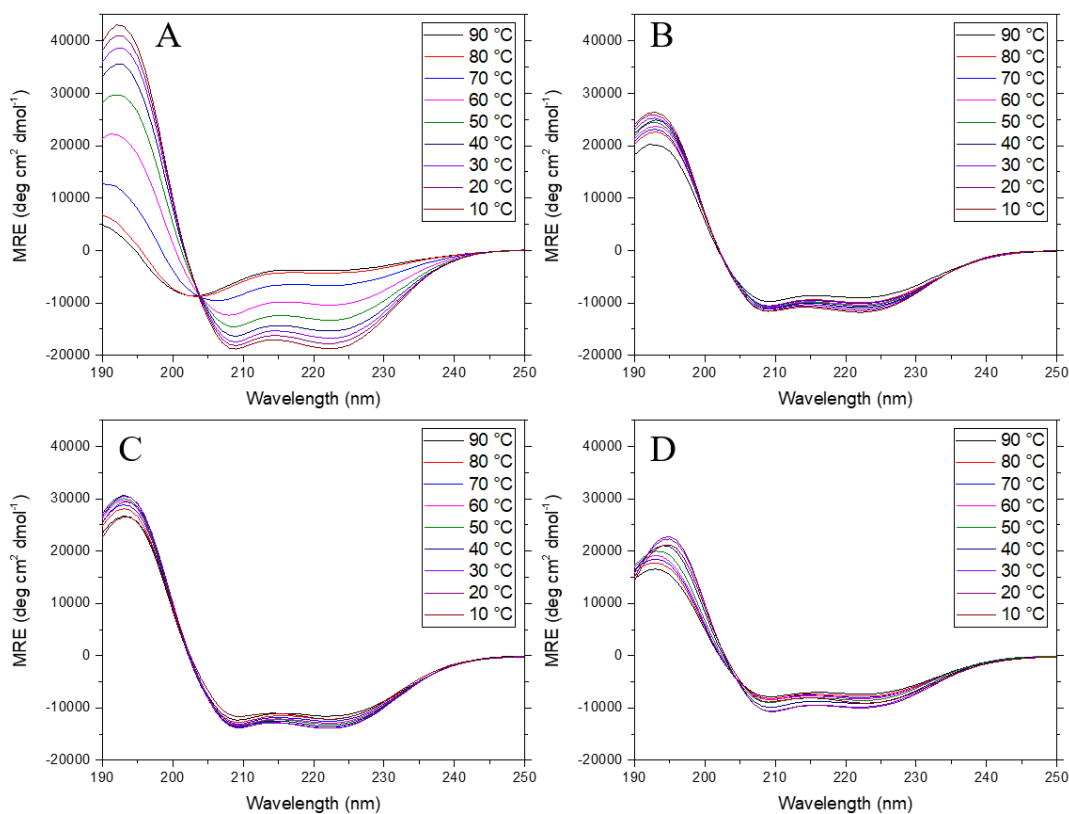


Figure 13 CD spectra showing the effects of initiator chain extension of the assembly behavior of the coiled-coil peptides. A) base peptide 4459-a-Br. B) 4459-a-E-Br. C) 4459-a-EG-Br. D) 4459-a-EGE-Br. Moving the bromide initiator group just one amino acid away from the base peptide sequence significantly increases the thermodynamic stability of the coiled-coil bundle. Additional amino acid additions show slight improvements. The increase in thermodynamic stability is hypothesized as resulting from the decrease in side chain interference with the inside assembly environment.

The chain extensions brought the assembly behavior back to the original behavior of 4459-a, showing evidence that the initiator arms were somehow interacting with the assembly that may have decreased their reactive activity. Polymerizations were conducted on these new set of peptides (labelled R<sub>104</sub>). However, similar polymerization behavior was observed as in the R<sub>102</sub> reactions, as shown in the MALDI spectra below.

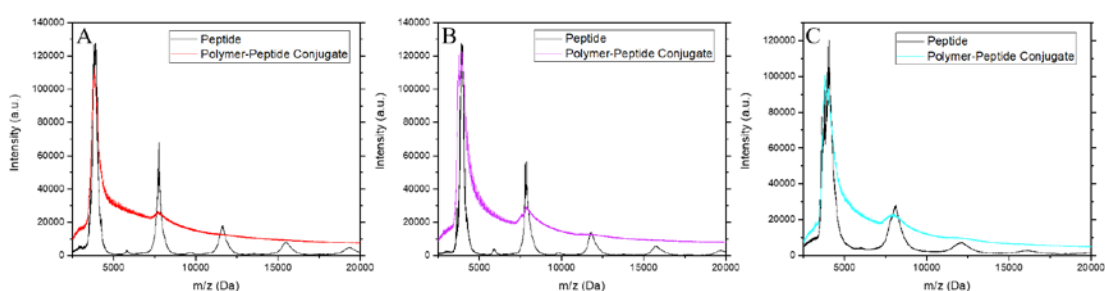


Figure 14 MALDI spectra of A) R<sub>104</sub>-1 B) R<sub>104</sub>-2 C)R<sub>104</sub>-3. While the chain extensions of the initiator proved to increase coiled-coil stability, there are no improvements in the polymerization conditions. For each of these reactions, the desired molecular weight was 18000 Da. This new population does not appear in the MALDI spectra.

Since the chain extension of the initiator did not successfully change the reaction results, changes in the reaction conditions were investigated in order to get a controlled polymerization. Aqueous ATRP reactions are notoriously hard to control, and there are many reports dedicated to investigating this.<sup>44-46</sup> The small molecule initiator was used to investigate changes in the next set of reactions; different ligands and salt concentrations were investigated (see Table 1 for the details). In Figure 15 below, the results of R<sub>106</sub> are displayed.

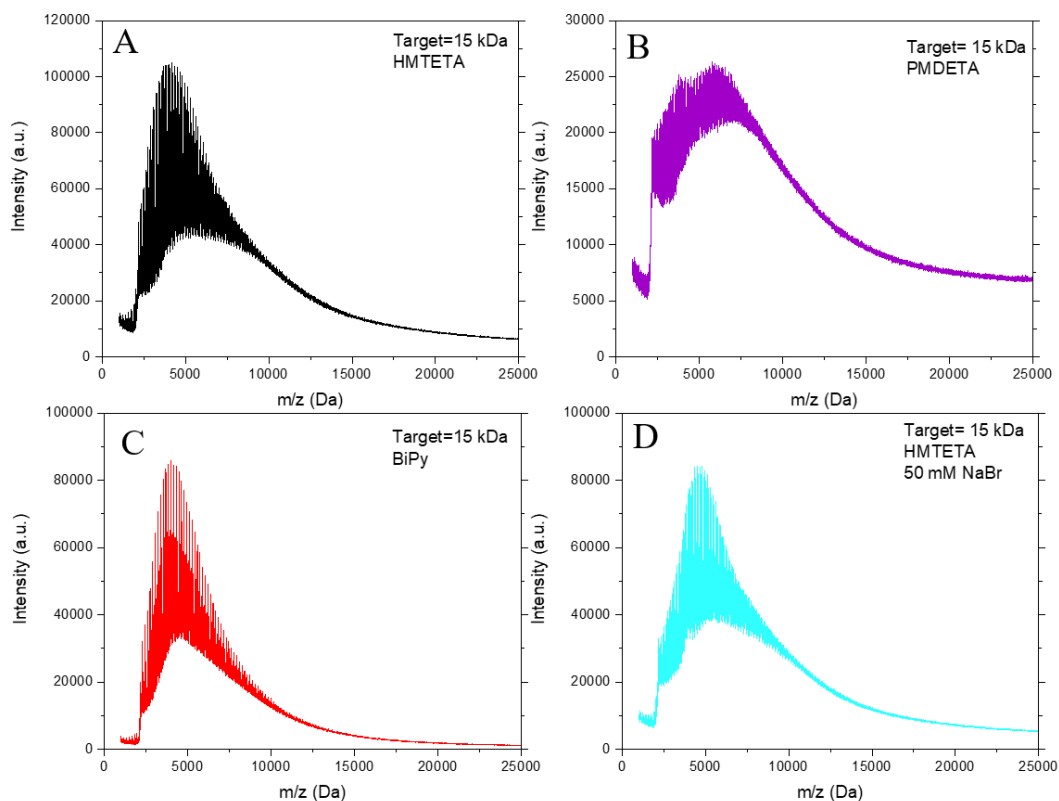


Figure 15 MALDI spectra of R<sub>106</sub>. All reactions targeted a molecular weight of 15 kDa. A) Typical reaction conditions B) PMDETA as the copper ligand C) BiPy as the copper ligand D) 50 mM sodium bromide

The results show slight improvements to the reaction, but similar results.

N,N,N',N'',N'''-pentamethyldiethylenetriamina (PMDETA) marginally increased the molecular weight of the polymer, but the dispersity deteriorates (Figure 15.B). Using 2,2'-Bipyridine (BiPy) as a ligand improved the distribution and size of p(DMAEMA) (Figure 15.C). Including sodium bromide as a salt to maintain a favorable equilibrium for polymerization increased the performance marginally (Figure 15.D). Overall, the polymerization was not proceeding as expected in the small molecule case, and the issues with polymerizing the macroinitiator are unresolved.

### 3.4 Summary and Conclusions

Different macroinitiators were prepared and the assembly behavior was analyzed; it was determined that extending the chain of the ATRP initiator away from the body of the assembly helps preserve the self-assembly behavior. Model polymerization studies were conducted with a small molecule ATRP initiator to determine the correct conditions for polymerizing DMAEMA. Many attempts at generating well defined polymer-peptide conjugates using the macroinitiator assemblies were shown, but no successful well defined conjugates were characterized.

Evidently, there are some issues with the polymerization conditions that need to be worked on. While the procedure was taken from literature, the system is not identical and the conditions may need to be adjusted.<sup>39</sup> Since the synthesis and purification of the macroinitiators are established, changing the initiator type may prove to be fruitless or uneconomical. Looking at changing the monomer to one that is more suitable for the initiator used may provide a more controlled polymerization. In addition, further studies at concentrations of initiator, copper/ligand, and salts could provide the correct conditions to successfully synthesize this conjugates.

In addition to determine better reaction conditions, different characterization techniques need to be developed to determine what is being synthesized. NMR can show conversions, but it is difficult to determine size with our current system. Size exclusion chromatography would provide a convenient and powerful system to get relative sizes, and should be pursued in future work. Finally, polyacrylamide gel electrophoresis techniques should allow for the relative and absolute measurements of peptides and their conjugates in the assembled and denatured form. With better synthetic and characterization procedures, the successful preparation of this conjugates should be accessible.

## Chapter 4

### CONCLUSIONS AND FUTURE DIRECTIONS

#### 4.1 Conclusions

A library of functionalized polypeptides that self-assemble into coiled-coil bundles were prepared and analyzed. These peptides are decorated with CuAAC and ATRP functionalities; in general, the addition of these motifs do not change the assembly behavior of the peptides, showing promise for utilizing this peptide motif in material design.

Attempts at covalent stabilization of the coiled-coil self-assemblies were presented but ultimately unsuccessful. It is difficult to ensure that the same small molecule reacts completely with one and only one peptide assembly. Some kind of secondary ordering or templating may be necessary to successfully realize covalent stabilization.

The efforts towards generating polymer-peptide conjugates showed promising results, but there is no conclusive evidence that the desired conjugate was synthesized. Issues with the access of the initiator were addressed by extending the initiator away from the assembly. Different parameters of the ATRP reaction were investigated to get the desired polymerization, but ultimately unsuccessful as of now.

Currently, the peptides prepared serve as an initial point to continue the investigation of different macromolecular geometries. More experiments need to be run to successfully prepare the desired geometries, and then materials need to be correctly characterized. Once these geometries are successfully synthesized, there are various studies that could come as a result of the novel materials being generated.

## 4.2 Future Directions – Physical Behavior of Novel Macromolecular Geometries

If the covalent stabilization is successful, the physical behavior of the resultant macromolecule can be studied to look at the assembly phenomena in novel ways. Upon heating, the melting temperature of the peptide assembly may shift higher; this suggests that the covalent bonds are able to hold the assemblies in place at higher energies. In addition, the covalent stabilization could increase the rate of self-assembly formation from a melted state, as all the components of the coiled-coil bundle are constantly near each other. Along with studying the thermal physical behavior of the system, this macromolecular architecture can now be studied in solvents other than water. Adding this macromolecule into a non-aqueous solvent and studying its physical behavior (whether it expands as sphere and fills with solvent or collapses and hides specific parts of the peptide) would lead to new understandings of entropically-restricted macromolecules and potential applications in controlled release and molecular capture.

If the peptide-polymer conjugate is successfully prepared, there are many physical phenomena that should be studied to elucidate conclusions about 1) the physical assembly of these systems and 2) the applications that these materials are suitable for. The first phenomenon to study is how the conjugates behave in solution at different concentrations. The polymers attached to the peptides will behave in solution differently depending on the amount that is in solution. This concentration behavior is a well-known phenomenon in polymer physics.<sup>47</sup> The addition of the self-assembled peptide may change the behavior.  $C^*$ , the concentration of polymer at which its physical shape in solution changes, could change due to the fact that the polymers entropy is restricted by its attachment to assembled bundles. Alternatively, the self-

assembly behavior of the core peptides could change once the physical behavior of the polymer changes at  $C^*$ . This would lead to fundamental understanding of the physical processes that dominate self-assembly behavior of polymer-peptide conjugates; this could have important impacts in understanding the limits of conjugation when post-modifying important proteins in biomedical applications.

Another parameter that probes the physical behavior of these conjugates is the temperature dependence of the system. In the current system, the self-assembled peptides have a melting temperature, and the monomer has an LCST: in this system,  $T_M > T_{LCST}$ . Slowly raising the solution temperature past the LCST would collapse the polymer chains onto each other as they become insoluble. The effects of this on the system can be studied to investigate 1) does the conjugation of the polymer to the peptide affect the normal phase behavior past the LCST and 2) will this phase change result in the disassembly of the peptides due to the entropic restraints that the LCST imposes on the system. Another temperature dependent test could involve heating the system above  $T_M$ , and then cooling the system at different rates. It is unknown whether the peptides will be able to reassemble upon cooling; this could depend on the chemistry and size of the polymer as well as the cooling rate. The failure of the self-assembly, if observed, could actually be used as an advantage. One can imagine a material that upon experiencing large local heating due to damage or system malfunction, the material would irreversibly disassemble, acting as a warning sensor. Studying the physical behavior of this conjugate system could provide fundamental and applied understandings to the use of these coiled-coil bundle conjugates.

### 4.3 Future Directions - Multi-Stimuli Responsive Hydrogels

If the conjugates described in this work were successfully prepared, they could be implemented into a cross-linked hydrogel that would offer unique properties. The proposed reaction scheme for the fabrication of this material is shown below in Figure 16.

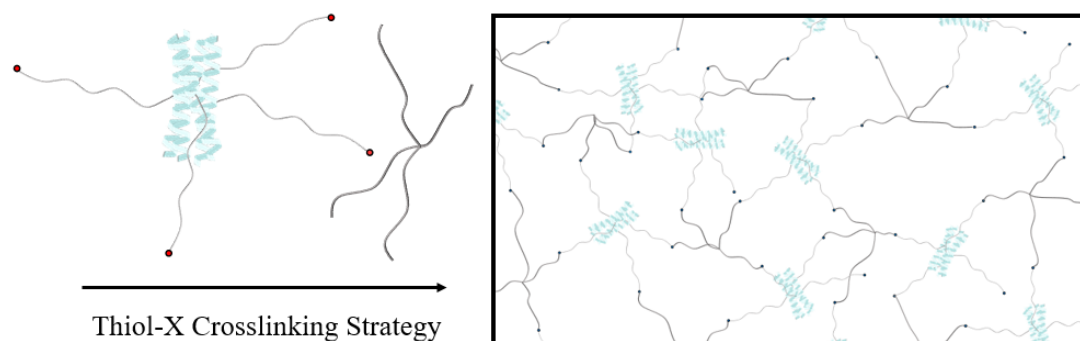


Figure 16 Reaction schematic detailing the synthesis of a cross-linked hydrogel incorporating the polymer-peptide conjugates. A flexible and hydrophilic tetrathiol could react with the prepared start conjugates to generate a crosslinked hydrogel, where the chemical crosslinks are generated by a thiol-X nucleophilic attack reaction. The physical crosslinks are the coiled-coil peptide assembly, which have temperature dependent behavior.

If the thiol-X reaction proposed proves to be problematic, there are a variety of methods described to produce end groups on ATRP polymers with click functionalities.<sup>27</sup> These can be combined with click hydrogel chemistries to create the desired material.<sup>48-50</sup> Synthesizing such a material is novel in its own right, but the physical understanding that can be obtained from studying the system is rich. First, there are two types of crosslinks in the same network, physical and chemical.

Investigating the dynamics of these crosslinks under stress could lead to better understandings of where material fatigue happens and where ultimate material failure happens. Perhaps of more interest would be the thermal behavior of this network. Tracking the mechanical properties of the material, such as the storage and loss moduli, as the LCST of the polymer and the melting temperature of the coiled-coil bundle is reached, would provide key insights into implementing these peptide motifs into materials. In addition, tracking the mechanical properties as the system is cooled through these transitions would tease out information about the self-assemblies inherent to the system. Ultimately, the proposed hydrogel would have many dynamic abilities, and could be used for building on the applications mentioned in the introduction on dynamic networks, chapter 1.5.

## REFERENCES

1. Vukusic, P.; Sambles, J. R. *Nature* **2003**, *424*, 852-856.
2. Bechert, D. W.; Bruse, M.; Hage, W.; Meter, R. *Naturwissenschaften* **2000**, *87*, 151-171.
3. Biro, L. P.; Vigneron, J. P. *Laser Photonics Rev.* **2011**, *5*, 27-51.
4. Huang, J.; Wang, X.; Wang, Z. L. *Nano Letters* **2006**, *6*, 2325-2331.
5. Dean, B.; Bhushan, B. *Phil. Trans. R. Soc. A* **2010**, *368*, 4774-4806.
6. Wen, L.; Weaver, J. C.; Lauder, G. V. *J. Exp. Bio.* **2014**, *217*, 1656-1666.
7. Autumn, K.; Liang, Y. A.; Hsieh, S. T.; Zesch, W.; Chan, W. P.; Kenny, T. W.; Fearing, R.; Full, R. J. *Nature* **2000**, *405*, 681-685.
8. Autumn, K.; Sitti, M.; Liang, Y. A.; Peattie, A. M.; Hansen, W. R.; Sponberg, S.; Kenny, T. W.; Fearing, R.; Israelachvili, J. N.; Full, R. J. *PNAS* **2002**, *99*, 12252-12256.
9. Liu, K.; Jiang, L. *Nano Today* **2011**, *6*, 155-175.
10. Sitti, M.; Fearing, R. S. *J. Adhesion Science Tech.* **2003**, *17*, 1055-1073.
11. Wegst, U. G. K.; Bai, H.; Saiz, E.; Tomsia, A. P.; Ritchie, R. O. *Nature Materials* **2014**, *14*, 23-36.
12. Lih, E.; Park, W.; Park, K. W.; Chun, S. Y.; Kim, H.; Joung, Y. K.; Kwon, T. G.; Hubbell, J. A.; Han, D. H. *ACS Cent. Sci.* **2019**, *5*, 458-467.
13. Gao, B.; Du, W.; Hao, Z.; Zhou, H.; Zou, D.; Zhang, R. *ACS Sustainable Chem. Eng.* **2019**, *7*, 5638-5648.
14. Bonderer, L. J.; Studart, A. R.; Gauckler, L. J. *Science* **2008**, *319*, 1069-1073.
15. Nelson, D. L.; Cox, M. M.; *Lehninger Principles of Biochemistry*, 7<sup>th</sup> ed.; W. H. Freedman & Co: New York, NY, 2017.
16. Dahiyat, B. I.; Mayo, S. L. *Science* **1997**, *278*, 82-87.
17. Haseltine, E. L.; Arnold, F. H. *Annual Rev. Biophysics and Biomolecular Structure* **2007**, *36*, 1-19.

18. Romero, P. A.; Arnold, F. H. *Nature Rev. Molecular Cell Biology* **2009**, *10*, 866-876.
19. Zhang, H. V.; Polzer, F.; Haider, M. J.; Tian, Y.; Villegas, J. A.; Kiick, K. L.; Pochan, D. J.; Saven, J. G. *Sci. Adv.* **2016**, *2*.
20. Macauley-Patrick, S.; Fazenda, M. L.; McNeil, B.; Harvey, L. M. *Yeast* **2005**, *22*, 249-270.
21. Sorensen, H. P.; Mortensen, K. K. *J. Biotech* **2005**, *115*, 113-128.
22. Connor, R. E.; Tirrell, D. A. *Polymer Reviews* **2007**, *47*, 9-28.
23. Hermanson, G. T. *Bioconjugate Techniques*, 3<sup>rd</sup> ed.; Elsevier: London, 2013.
24. Montabetti, C. A. G. N.; Falque, V. *Tetrahedron* **2005**, *61*, 10827-10852.
25. Braunecker, W. A.; Matyjaszewski, K. *Progress in Polymer Science* **2007**, *32*, 93-146.
26. Patten, T. E.; Matyjaszewski, K. *Adv. Mater.* **1998**, *10*, 901-915.
27. Matyjaszewski, K.; Tsarevsky, N. V. *Nature Chemistry* **2009**, *1*, 276-288.
28. Siegwart, D. J.; Oh, J. K.; Matyjaszewski, K. *Progress in Polymer Science* **2011**, *37*, 18-37.
29. Yokoyama, M.; Miyauchi, M.; Yamada, N.; Okano, T.; Sakurai, Y.; Kataoka, K.; Inoue, S. *J. Control Release* **1990**, *11*, 269-278.
30. Xu, M.; Evans Jr, T. C. *Methods* **2001**, *24*, 257-277.
31. Kolb, H. C.; Finn, M. G.; Sharpless, K. B. *Angew. Chemie Int. Ed.* **2001**, *40*, 2004-2021.
32. Best, M. D. *Biochemistry* **2009**, *48*, 6571-6584.
33. Xi, W.; Scott, T. F.; Kloxin, C. J.; Bowman, C. N. *Adv. Func. Mater.* **2014**, *24*, 2572-2590.
34. Hoffman, A. S. *Adv. Drug Delivery Rev.* **2002**, *54*, 3-12.
35. Bajpai, A. K.; Shukla, S. K.; Bhanu, S.; Kankane, S. *Progress in Polymer Science* **2008**, *33*, 1088-1118.

36. Kharkar, P. M.; Kiick, K. L.; Kloxin, A. M. *Chem. Soc. Rev.* **2013**, *42*, 7335-7372.
37. Almeida, M.; O'Brien, C. A. *J. Gerontol. A: Biol. Sci. Med. Sci.* **2013**, *68*, 1197-1208.
38. Song, H. B.; Baranek, A.; Bowman, C. N. *Polym. Chem.* **2016**, *7*, 603-612.
39. Murata, H.; Cummings, C. S.; Koepsel, R. R.; Russell, A. J. *Biomacromolecules* **2013**, *14*, 1919-1926.
40. Collier, J. H.; Messersmith, P. B. *Adv. Mater.* **2004**, *16*, 907-910.
41. Du, A. W.; Stenzel, M. H. *Biomacromolecules* **2014**, *15*, 1097-1114.
42. Harris, J. M.; Chess, R. B. *Nature Rev. Drug Discovrey* **2003**, *2*, 214-221.
43. Murata, H.; Carmali, S.; Baker, S. L.; Matyjaszewski, K.; Russell, A. J. *Nature Comm.* **2018**, *9*, 1-10.
44. Fantin, M.; Isse, A. A.; Gennaro, A.; Matyjaszewski, K. *Macromolecules* **2015**, *48*, 6862-6875.
45. Simakova, A.; Averick, S. E.; Konkolewicz, D.; Matyjaszewski, K. *Macromolecules* **2012**, *45*, 6371-6379.
46. Wright, T. A.; Page, R. C.; Konkolewicz, D. *Polym. Chem.* **2019**, *10*, 434-454.
47. Rubinstein, M.; Colby, R. H. *Polymer Physics*. Oxford University Press: Oxford, UK, 2003.
48. Malkoch, M.; Vestberg, R.; Gupta, N.; Mespouille, L.; Dubois, P.; Mason, A. F.; Hedrick, J. L.; Liao, Q.; Frank, C. W.; Kinsbury, K.; Hawker, C. J. *Chem. Comm.* **2006**, *26*, 2774-2776.
49. DeForest, C. A.; Anseth, K. S. *Nature Chemistry* **2011**, *3*, 925-931.
50. Jiang, Y.; Chen, J.; Deng, C.; Suuronen, E. J.; Zhong, Z. *Biomaterials* **2014**, *35*, 4969-4985.

## Appendix A

### PEPTIDE SEQUENCES

Table 2 Peptide sequences used with corresponding experimental relevance

Peptide	Sequence	Notes
Diazide	KEEIRRMA EEIRKMA ERIQQMA EQIQQEK	Used to generate the coiled-coil bundle in the stabilization studies.
P622-Br	DEKIKNM ADQIKKM AWMIDRM AEKIDREA	Initially investigated as a potential macroinitiator, but assembly properties were questionable.
4459-a-Br	DEEIRRMA EEIRKMA ERIQQMA EQIQQEA	Used as the initial macroinitiator
4459-a-E-Br	DEEIRRMA EEIRK-(branch-E)-MA ERIQQMA EQIQQEA	One amino-acid extension of the ATRP initiator away from the bundle.
4459-a-EG-Br	DEEIRRMA EEIRK-(branch-EG)-MA ERIQQMA EQIQQEA	Two amino-acid extension of the ATRP initiator away from the bundle.
4459-a-EGE-Br	DEEIRRMA EEIRK-(branch-EGE)-MA ERIQQMA EQIQQEA	Three amino-acid extension of the ATRP initiator away from the bundle.

## Appendix B

### SUPPORTING INFORMATION: COVALENT STABILIZATION OF THE COILED-COIL MOTIF

Table 3 CuAAC reaction conditions for covalent stabilization of coiled-coil assembly

Attempt 1	MW (g/mol)	$\mu\text{mol}$	Equivalents	Concentration (mM)
Diazido-Peptide	4042	0.223	1	2
Tetraalkyne	288	0.445	2	4
CuSO <sub>4</sub>	159.6	0.111	1	2
NaAsc	198	0.445	4	8
THPTA	434.5	0.223	2	4
Attempt 2				
Diazido-Peptide	4042	0.223	1	5
Tetraalkyne	288	0.445	1.2	4
CuSO <sub>4</sub>	159.6	0.111	0.5	1
NaAsc	198	0.445	2	4
THPTA	434.5	0.223	1	2

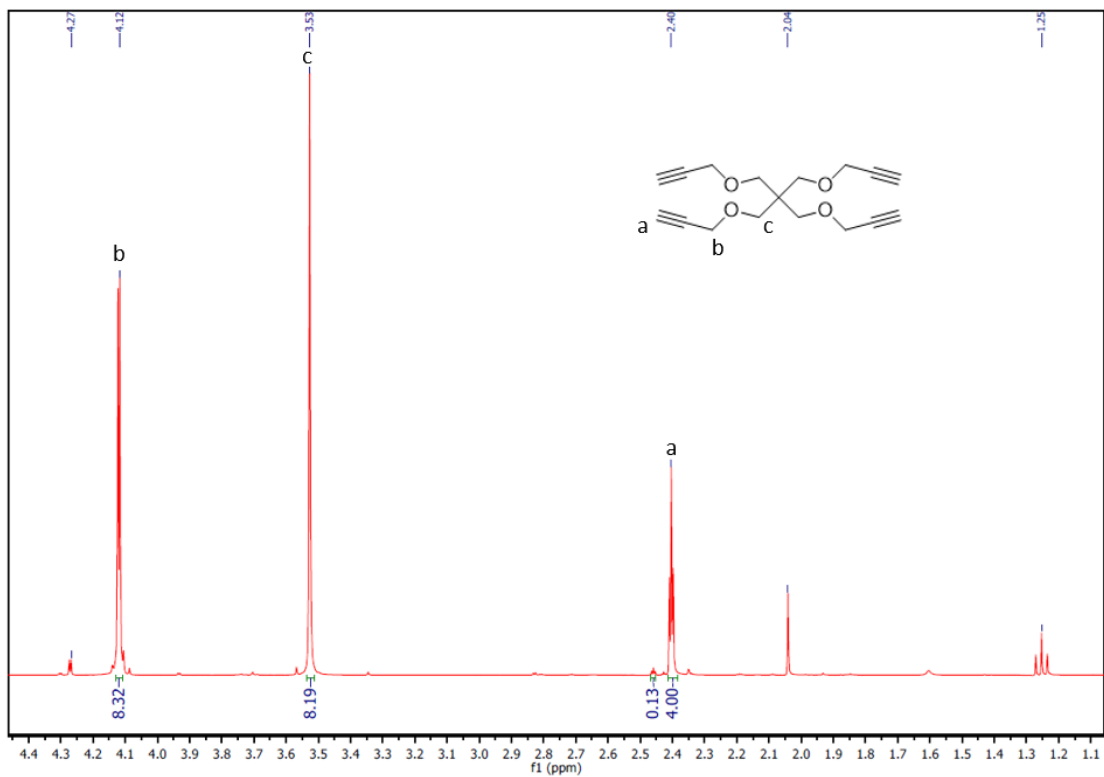


Figure 17 NMR spectrum of the tetraalkyne small molecule used for covalent stabilization.

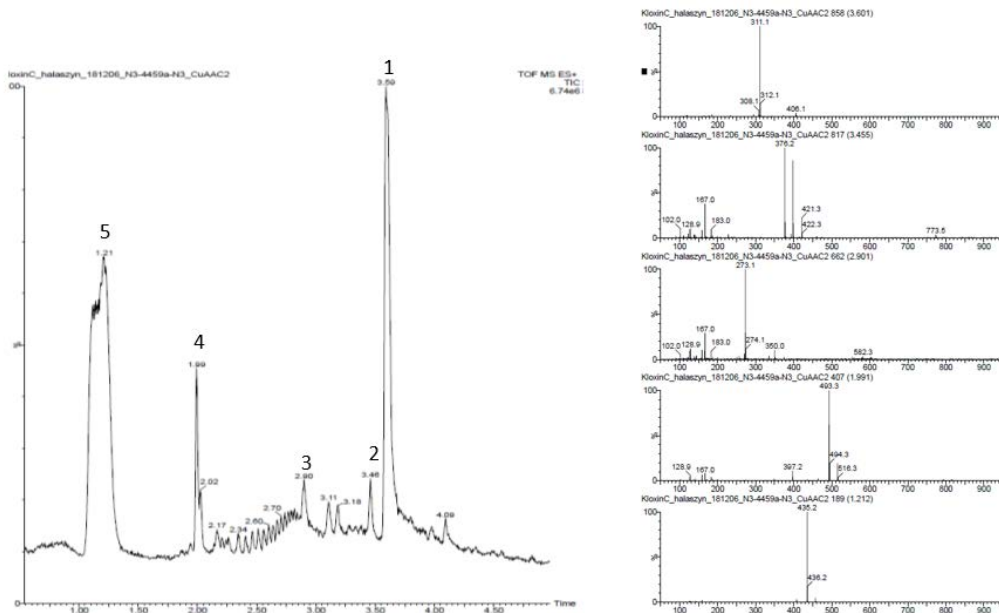


Figure 18 Chromatogram and corresponding mass spectra for the first covalent stabilization reaction attempt.

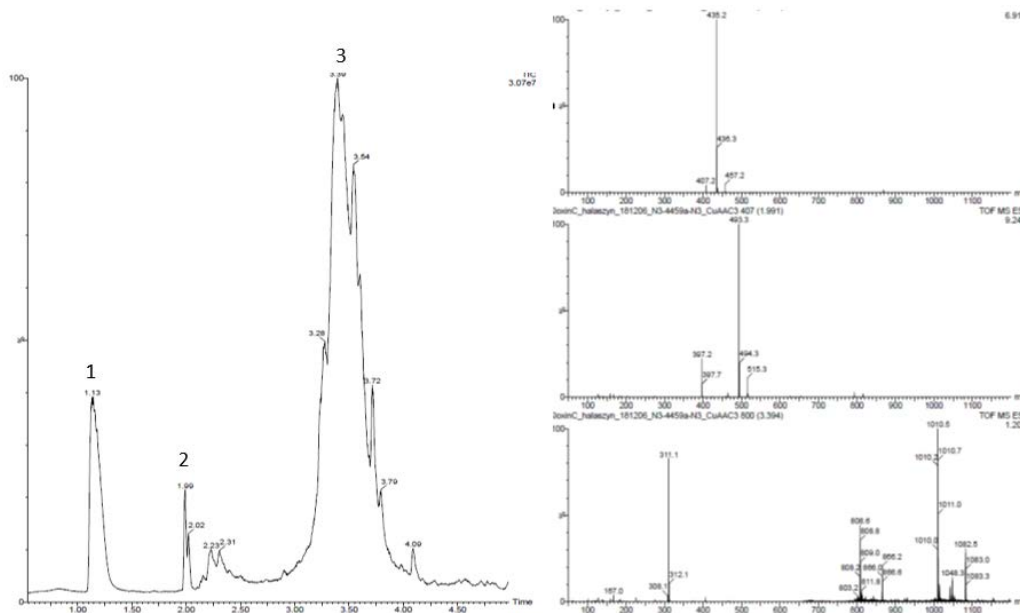


Figure 19 Chromatogram and corresponding mass spectra for the second covalent stabilization reaction attempt.

## Appendix C

### SUPPORTING INFORMATION: SYNTHESIS OF POLYMER-PEPTIDE CONJUGATES WITH STAR GEOMETRIES

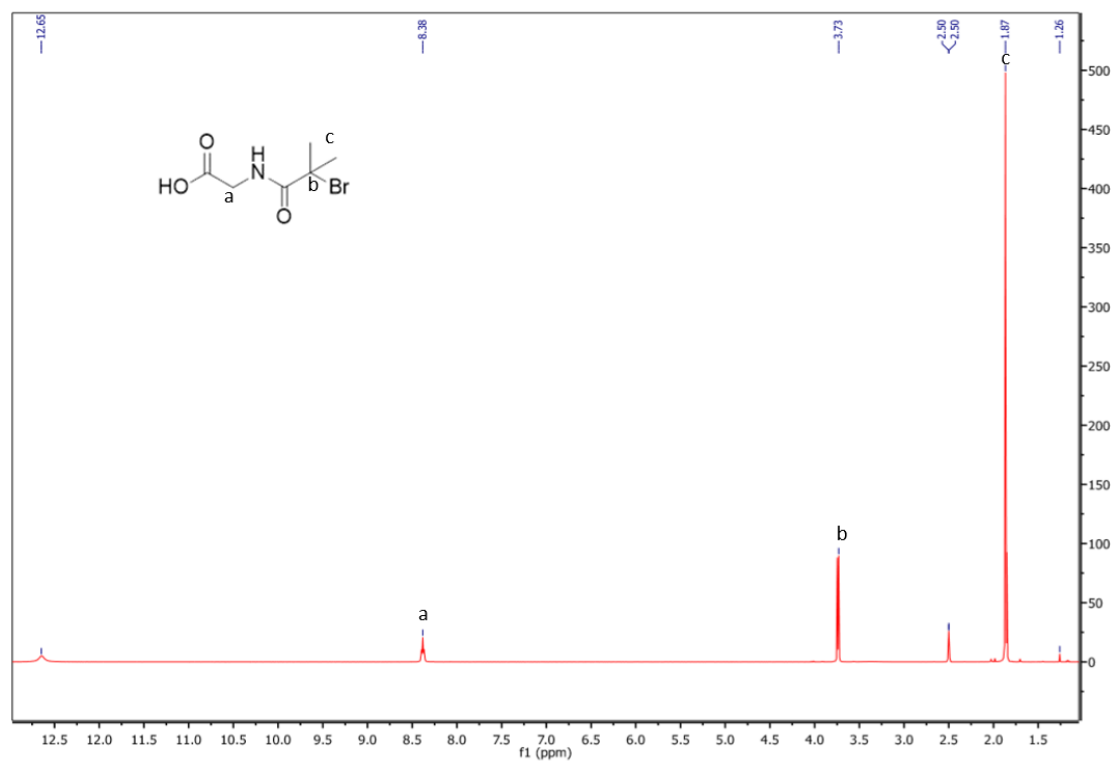


Figure 20 NMR spectrum of the small molecule initiator used in the model polymerizations (sample prepared in deuterated DMSO).

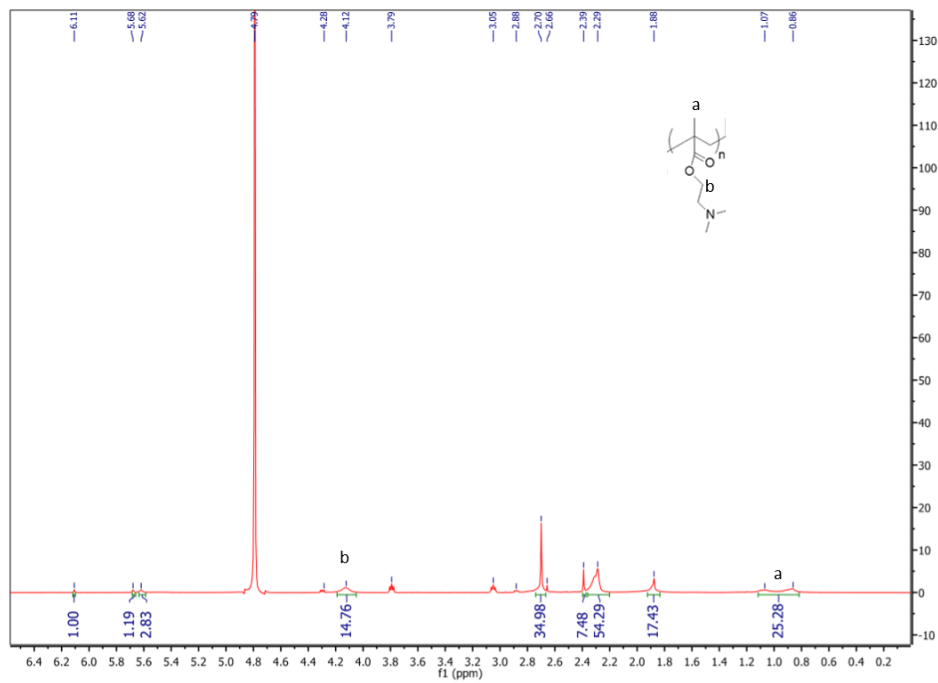


Figure 21 NMR spectrum of R95-1.

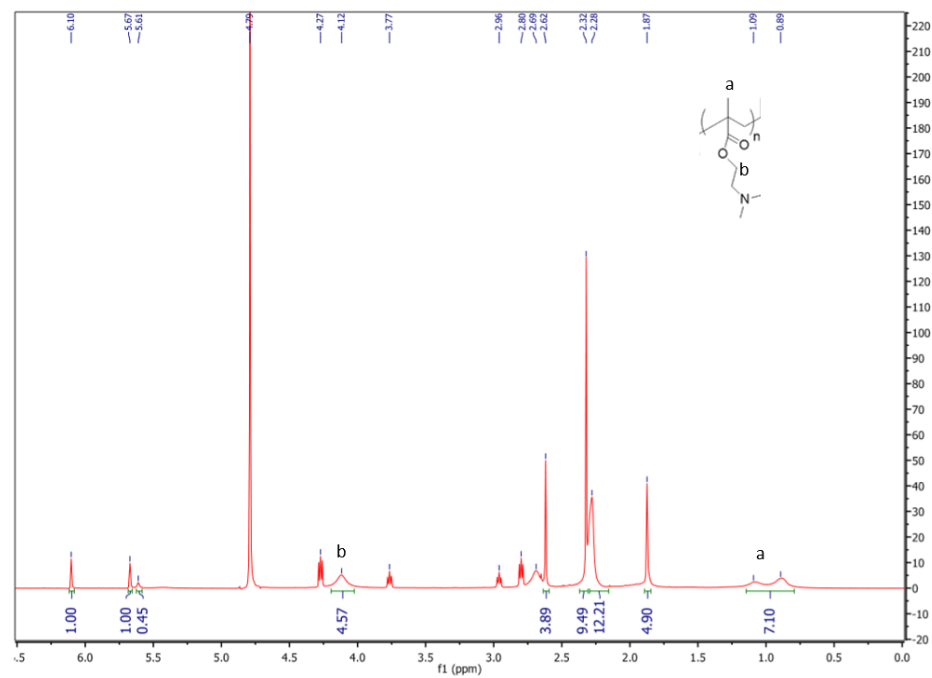


Figure 22 NMR spectrum of R95-3

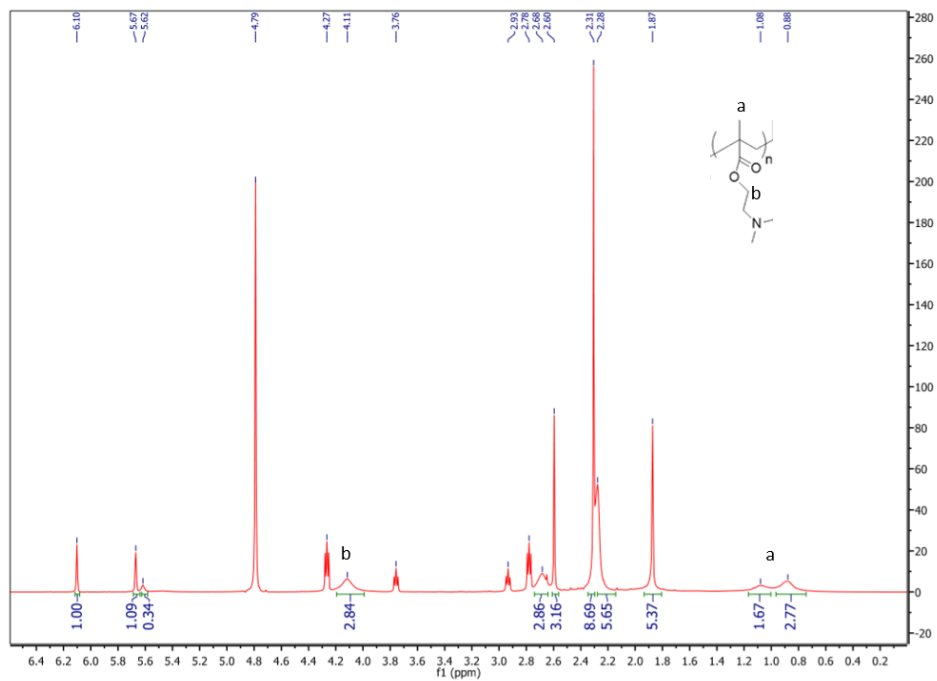


Figure 23 NMR spectrum of R<sub>95-4</sub>

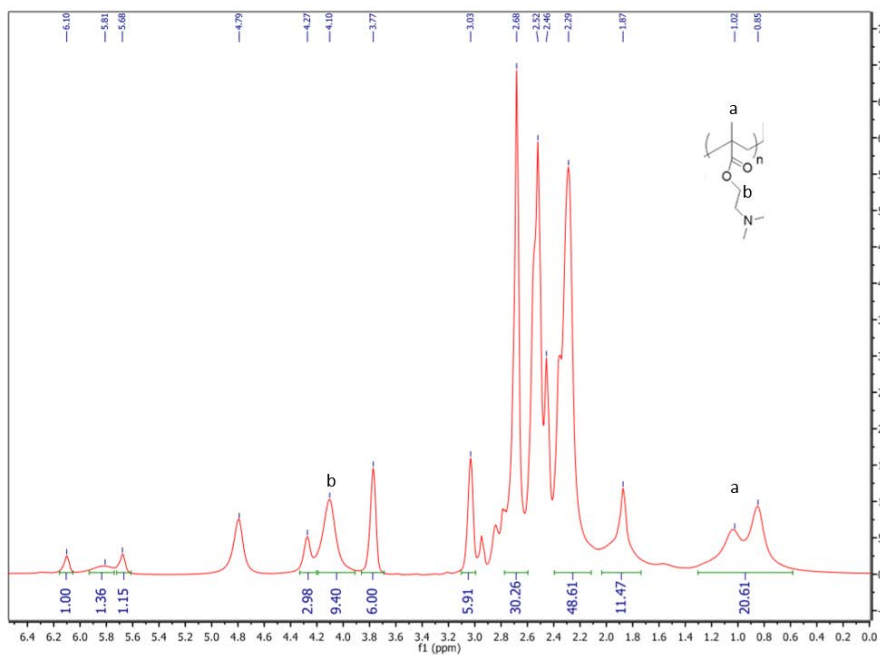


Figure 24 NMR spectrum of R<sub>98-1</sub>

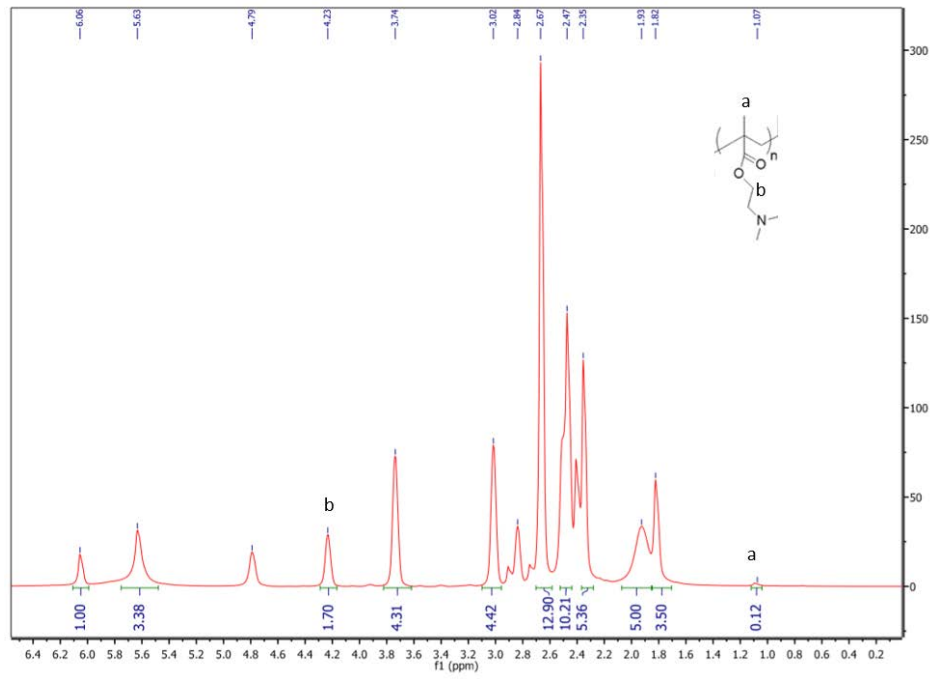


Figure 25  $^1\text{H}$  NMR spectrum of R98-2

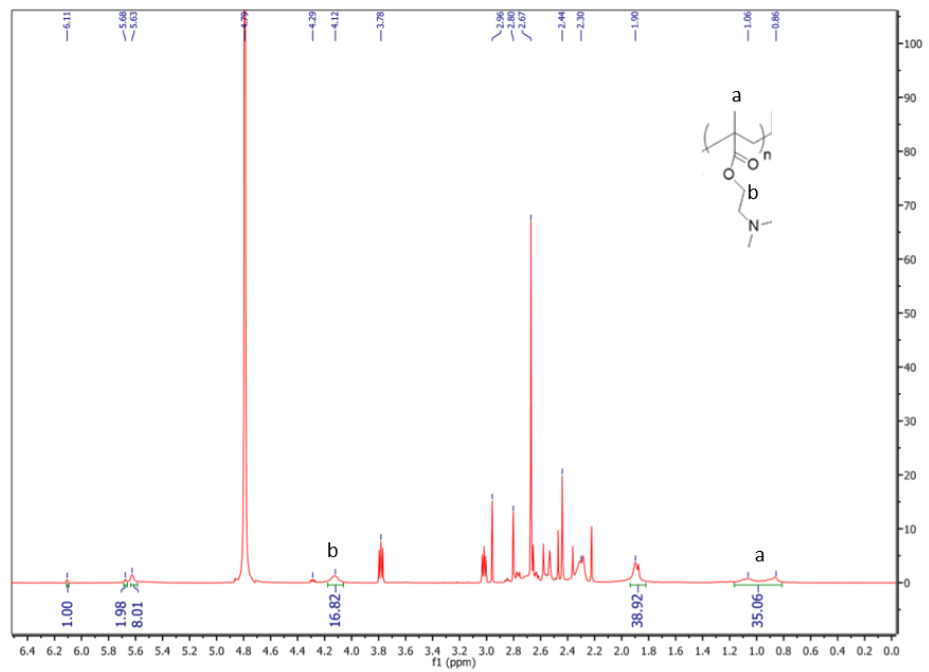


Figure 26  $^{13}\text{C}$  NMR spectrum of R98-3

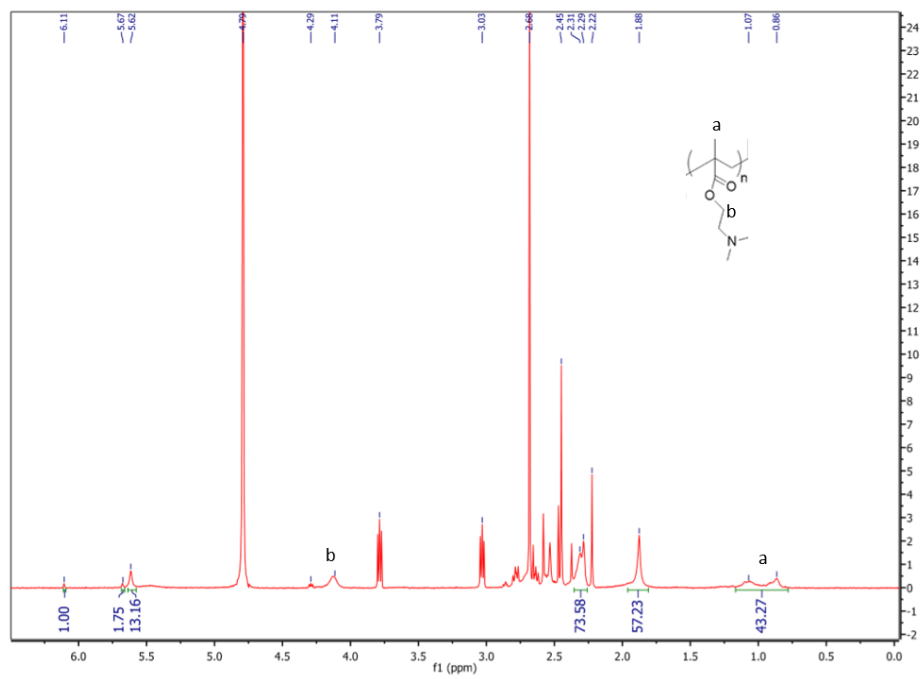


Figure 27 NMR spectrum of R100-1.

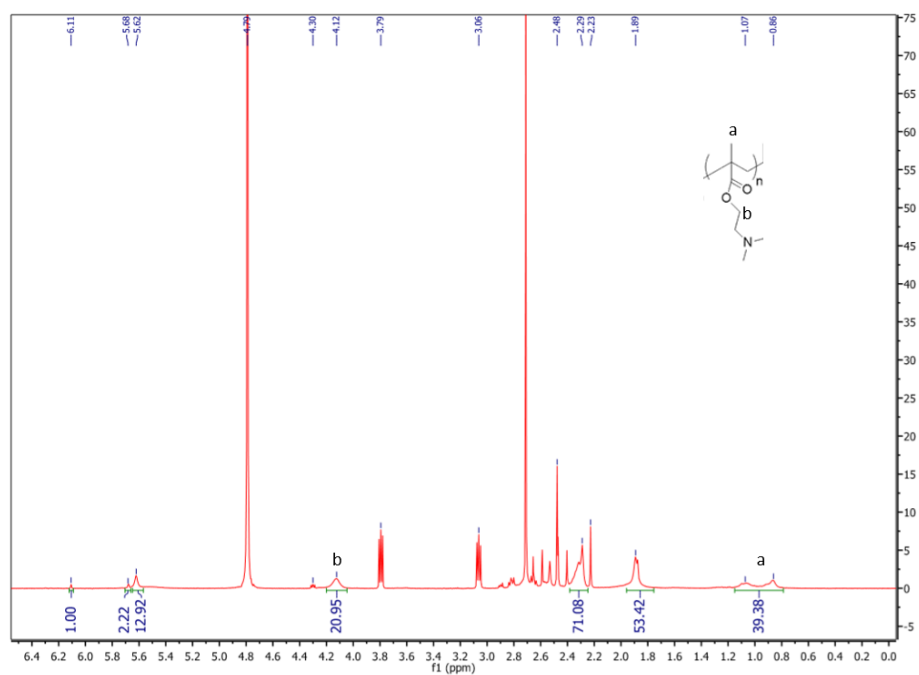


Figure 28 NMR spectrum of R100-2.

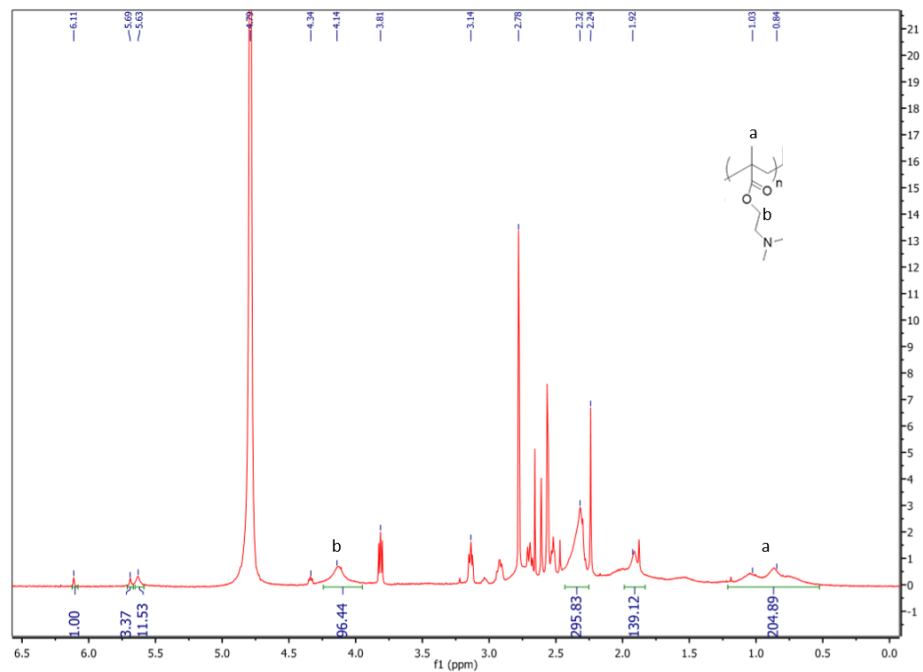


Figure 29 NMR spectrum of R<sub>100</sub>-4.

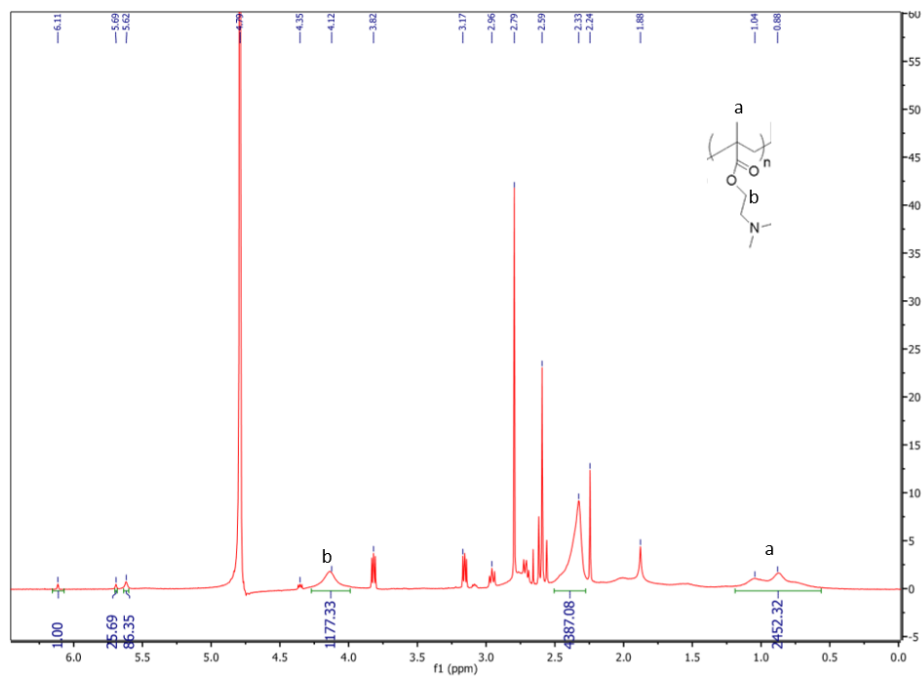


Figure 30 NMR spectrum of R<sub>102</sub>-1.

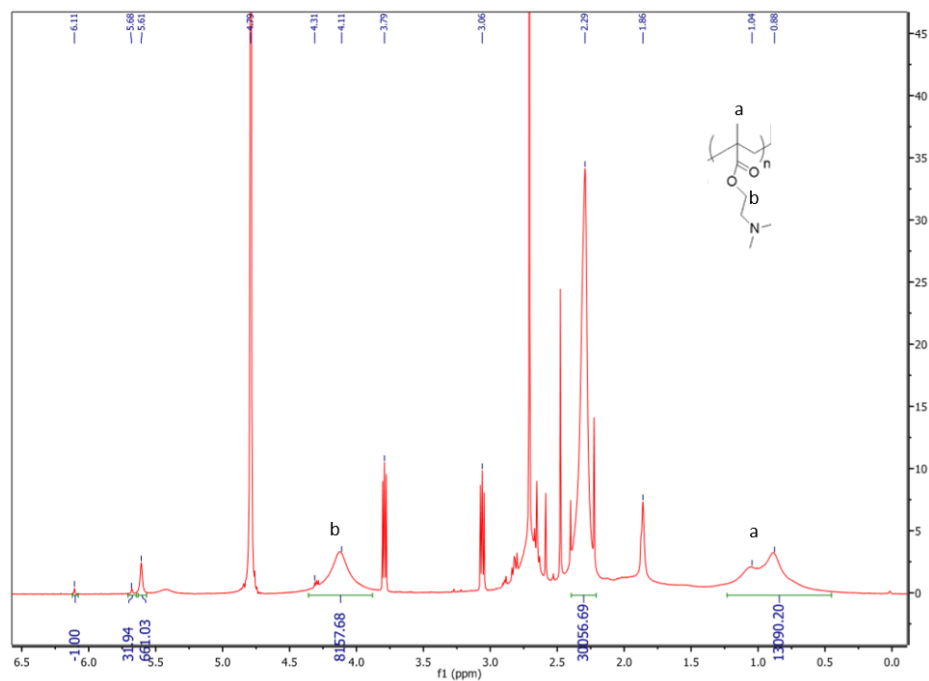


Figure 31 NMR spectrum of R<sub>102</sub>-2.

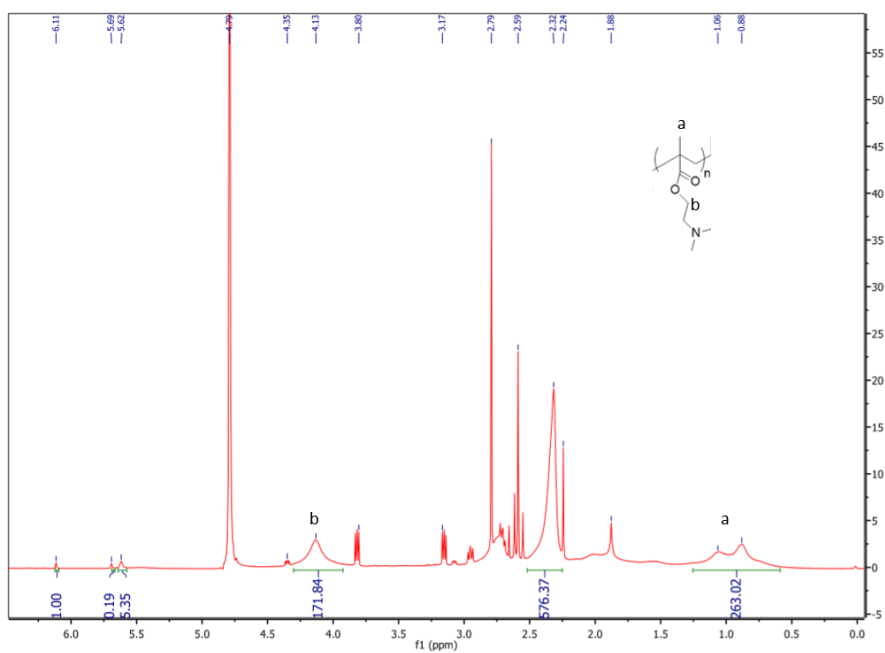


Figure 32 NMR spectrum of R<sub>102</sub>-3.

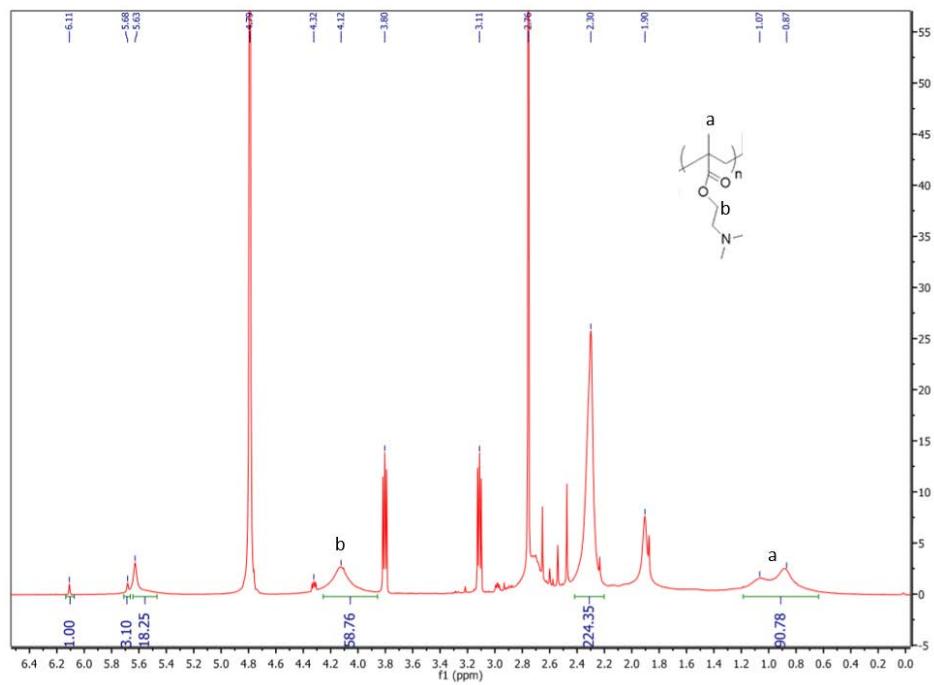


Figure 33 NMR spectrum of R104-1.

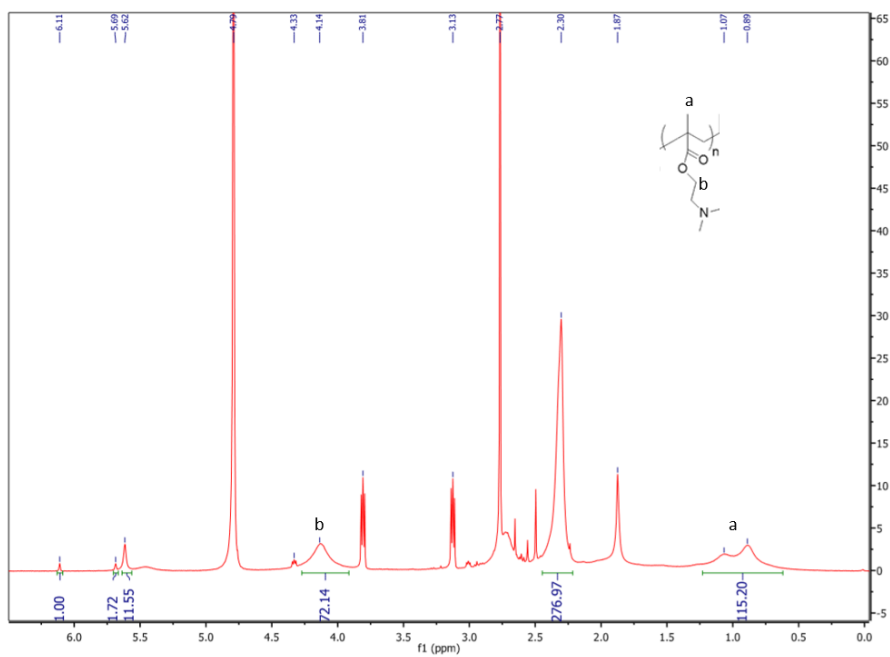


Figure 34 NMR spectrum of R104-2

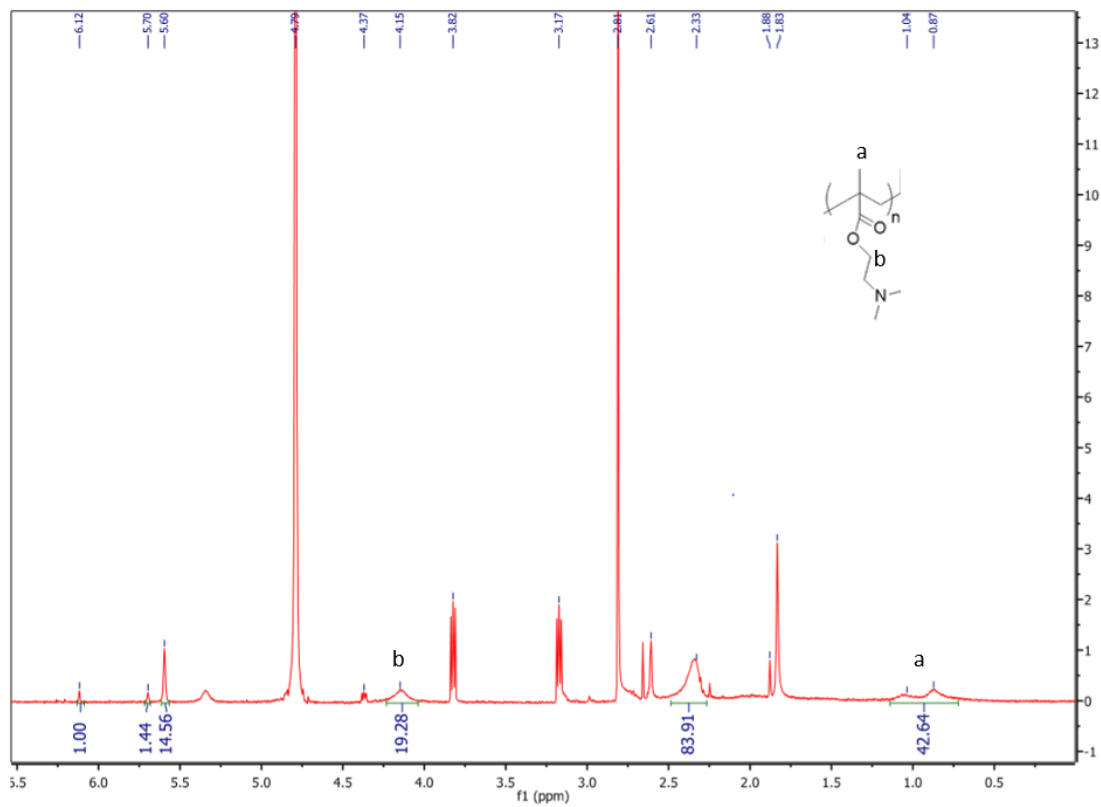


Figure 35 NMR spectrum of  $R_{104-3}$ .